



# Greenhouse gas emissions from compacted peat soil

---

Antonia Barbara Daniela Hartmann

Independent project 30 hp

Swedish University of Agricultural Sciences, SLU

Department of Soil and Environment

EnvEuro - European Master in Environmental Science

Uppsala, 2021





# Greenhouse gas emissions from compacted peat soil

Antonia Hartmann

<b>Supervisor</b>	Dr. Örjan Berglund, SLU, Department of Soil and Environment
<b>Assistant Supervisor</b>	Daniel Iseskog, SLU, Department of Soil and Environment
<b>Assistant Supervisor</b>	Dr. Sabine Jordan, SLU, Department of Soil and Environment
<b>Assistant Supervisor</b>	Prof. Dr. Thilo Streck, University of Hohenheim, Department of Biogeophysics
<b>Examiner</b>	Prof. Dr. Björn Lindahl, SLU, Department of Soil and Environment
<b>Credits</b>	30 hp
<b>Level</b>	Second cycle, A2E
<b>Course title</b>	Master thesis in Environmental science
<b>Course Code</b>	EX0897
<b>Programme</b>	EnvEuro - European Master in Environmental Science
<b>Course coordinating dept.</b>	Soil and Environment
<b>Place of publication</b>	Uppsala, Sweden
<b>Year of publication</b>	2021
<b>Keywords</b>	Carbon dioxide / Compression index / Peatland agriculture / Recompression index / Sand addition / Soil compaction

**Swedish University of Agricultural Sciences, SLU**

Faculty of Natural Resources and Agricultural Sciences (NJ)

Department of Soil and Environment

## **Publishing and Archiving**

- YES, I hereby give permission to publish the present thesis in accordance with the SLU agreement regarding the transfer of the right to publish a work.
- NO, I do not give permission to publish the present work. The work will still be archived and its metadata and abstract will be visible and searchable.

## **Abstract**

Cultivated peat soils are a main driver for CO<sub>2</sub> and N<sub>2</sub>O emissions, while the gas fluxes are dependent on intrinsic soil properties and land use. Sand addition into peat soils might reduce greenhouse gas (GHG) emissions and enhance soil strength, and thus the ability to tolerate soil compaction. Soil compaction due to vehicular traffic leads to a decrease in aeration and changes in water flow, which might alter microbial activity and gas flow. The goal of this thesis was to investigate how soil compaction with different stress levels and sand addition affect soil physical properties and GHG emissions of peat soils. Incubator measurements three days before and after compaction were used to analyze the effect of soil compaction, which was conducted in a uniaxial compression machine. Furthermore, a new method was developed to observe the dynamics of gas fluxes during compaction. Field measurements complemented the laboratory study to determine the effect of sand addition. The compressive behaviour of peat soils was examined using the compression ( $C_c$ ) and recompression index ( $C_s$ ) which are measures for soil compressibility and rebound after stress release. This study shows reduction of CO<sub>2</sub> emissions after compaction. However, this effect might be due to the high initial water-filled pore space and at lower water contents, compaction might have the opposite effect on GHG emissions. Higher mechanical loading had an effect on CO<sub>2</sub> fluxes, while the trend was unclear and seems to be dependent on water content. Methane fluxes were below the detection limit and compaction might lead to hot moments in N<sub>2</sub>O emission. Sand addition reduced CO<sub>2</sub> emissions and influenced the compressive behaviour of peat soils by reducing soil compressibility but also rebound. Linear relationships between soil mechanical properties and initial void ratio were found, indicating the high dependency of mechanical behaviour on intrinsic soil properties. In conclusion, sand addition might be a good agricultural management practise for cultivated peat soils, while the impact of soil compaction on GHG emissions under different moisture regimes has to be further assessed. This pilot study, emphasizes a need of further research to improve understanding the influencing factors of vehicular traffic as well as sand addition on GHG emissions and soil mechanical properties of cultivated peat soils.

## **Popular-scientific summary**

Peatlands store the majority of the global carbon stocks and are mainly managed for agriculture and forestry. This management includes the lowering of groundwater levels (drainage) and fertilization, which leads to changes in soil properties and the microbial activity in the soil. Therefore, cultivated peat soils are a main driver for greenhouse gas (GHG) emissions like carbon dioxide and nitrous oxide and in order to reduce its climate impact, a sustainable management of cultivated peat soils is needed. Therefore, more research has to be conducted to find applicable solutions as well as to understand the impact of current agricultural practices on GHG emissions. A common practice is to mix sand into the upper part of peat soils to improve crop growth and soil strength, thus the ability to tolerate soil compaction. This reduces the risk of tractors to sink in. Sand addition changes the soil composition and affects soil properties like water and air flow in the soil, which could lead to lower GHG emissions. Vehicular traffic compresses the soil and reduces the amount of air-filled pores in the soil. This might influence the microbial activity and gas fluxes between soil and atmosphere. The goal of this thesis was to investigate how soil compaction with different pressures and sand addition affects soil properties and GHG emissions of peat soils. Furthermore, indicators for soil compressibility and rebound after stress release were analyzed to understand the impact of vehicular traffic on peat with and without sand addition. In the laboratory, soil samples were compacted in a compression machine at different compaction pressures to simulate vehicular traffic. A new method was developed to measure the dynamics of GHGs during and shortly after compaction. This method gives the opportunity to investigate direct changes in GHG fluxes, while incubator measurements three days before and after compaction investigates the influence of compaction over a longer period. Field measurements complemented the incubator experiment to assess the influence of sand addition on GHG fluxes. The study shows that carbon dioxide emissions were lower when soil was compacted while nitrous oxide emissions only occurred after compaction. This might be due to high initial water contents and at lower water contents, which is more realistic for field conditions, compaction could have the opposite effect. Higher compaction pressure influenced carbon dioxide emissions, but the trend was unclear and seemed to be dependent on water content. Sand addition reduced carbon dioxide emissions, reduced soil compressibility but also rebound. In conclusion, sand addition might be a good management practice for cultivated peat soils, while the impact of soil compaction on GHG emissions at different water contents has to be evaluated in the future. This pilot study emphasizes a need for further research to improve understanding the influencing factors of vehicular traffic as well as sand addition on GHG emissions and soil mechanical properties of cultivated peat soils.

# Contents

<b>List of Figures</b>	<b>i</b>
<b>List of Tables</b>	<b>iv</b>
<b>List of Abbreviations</b>	<b>vi</b>
<b>1 Introduction</b>	<b>1</b>
1.1 GHG emission of peat soils . . . . .	2
1.2 Influence of sand addition on GHG emission . . . . .	2
1.3 Influence of soil compaction on GHG emissions . . . . .	3
1.4 Compressive behaviour of peat soils . . . . .	3
1.5 Hypotheses . . . . .	5
<b>2 Material &amp; Methods</b>	<b>6</b>
2.1 Field design and field site description . . . . .	6
2.2 Field measurements . . . . .	8
2.3 Soil sampling and preparation . . . . .	9
2.4 Description of the compaction experiment . . . . .	9
2.5 Incubator measurements . . . . .	10
2.6 Measurement of GHG dynamics during compaction . . . . .	11
2.7 Measurement of chemical and physical properties . . . . .	13
2.8 Mechanical behaviour of peat soil . . . . .	15
<b>3 Results</b>	<b>16</b>
3.1 Field measurements . . . . .	16
3.2 Incubator measurements . . . . .	16
3.2.1 Influence of sand addition on CO <sub>2</sub> fluxes . . . . .	17
3.2.2 Influence of soil compaction on CO <sub>2</sub> fluxes . . . . .	19
3.2.3 Influence of different mechanical loading on CO <sub>2</sub> fluxes . . . . .	19
3.2.4 Influence of soil compaction on N <sub>2</sub> O fluxes . . . . .	21
3.3 GHG dynamics during compaction . . . . .	21
3.4 Influence of compaction on physical properties . . . . .	21

3.5	Mechanical properties . . . . .	24
<b>4</b>	<b>Discussion</b>	<b>26</b>
4.1	Influence of sand addition on CO <sub>2</sub> emissions . . . . .	26
4.2	Influence of soil compaction on CO <sub>2</sub> emissions . . . . .	26
4.3	Influence of different mechanical loading on CO <sub>2</sub> fluxes . . . . .	28
4.4	Influence of soil compaction on N <sub>2</sub> O fluxes . . . . .	29
4.5	Improvement of GHG measurements during compaction . . . . .	29
4.6	Mechanical behaviour of peat soils . . . . .	30
<b>5</b>	<b>Conclusions</b>	<b>31</b>
	<b>Acknowledgments</b>	<b>32</b>
	<b>Supplementary Material</b>	<b>32</b>
	<b>References</b>	<b>36</b>

## List of Figures

- 1 Left: Measured compression curve described by void ratio ( $e$ ) as a function of the logarithm of applied stress ( $\sigma$ ). Right: Idealised compression behaviour of soil which is plastic and irreversible along the virgin compression line (VCL) and elastic and reversible along the swelling line (SL). Slopes of VCL and SL are termed compression index  $C_c$  and recompression index  $C_s$  (Keller et al. 2011). . . . . 5
- 2 Left: The field experiment at Broddbo has a randomized block design with different amounts of sand additions. A represents the control plot (turquoise), B 2.5 cm foundry sand (white) and C 5 cm foundry sand (orange) mixed into 10-15 cm topsoil. Each plot is 8 m by 4 m and is vegetated with timothy (*Phleum pratense*). Right: GHG flux measurement with manual opaque chamber and Gasmeter GT5000 Terra portable gas analyzer. (Photo: Antonia Hartmann). . . . . 7
- 3 Left: GHG flux measurements with air-tight polypropylene jar (incubator) and Gasmeter GT5000 Terra portable gas analyzer Right: Measurement of the displacement height after compaction for exact calculation of the soil physical properties and air volume for GHG flux calculation (Photos: Antonia Hartmann). . . . . 11
- 4 a) Piston with porous cap and channels through piston core. b) Piston position on soil surface, rubber seals air-tight around piston. c) Tube system connected to piston and integrated valves. Valves on the left side were only open during flushing with soda lime. d) Whole setup of the uniaxial compression machine with a tube connection between piston and GHG analyzer for gas measurements. . . . . 12
- 5 Increase of CO<sub>2</sub> concentration was 33.3 ppm within 10 minutes after removing ambient CO<sub>2</sub> using soda lime. Therefore, leakage of tubes can be neglected in compaction experiments. . . . . 13
- 6 Mean CO<sub>2</sub> flux and standard deviations of field measurements during calendar week 16-28. Each point represents 3 measuring points per plot treatment. Triangle and dotted bars indicate soil temperature [°C]. CO<sub>2</sub> flux of control A (turquoise) was statistically different from C (orange,  $p = 0.0431$ ). CO<sub>2</sub> fluxes were highly dependent on soil temperature ( $p < 0.0001$ ). Significant p-values of ANOVA using a linear mixed effect (lme) model: \*\*\*  $< 0.001$ , \*\*  $< 0.01$ , \*  $< 0.05$ . . . . . 16

7 Mean CO<sub>2</sub> flux and standard deviations of field measurements during calendar week 16-28. Each point represents 3 measuring points per plot treatment. Triangle and dotted bars indicate VWC [%]. CO<sub>2</sub> flux of control A (turquoise) was statistically different from C (orange, p = 0.0431). No statistical effect between VWC and CO<sub>2</sub> fluxes was found. Significant p-values of ANOVA using a linear mixed effect (lme) model: \*\*\* < 0.001, \*\* < 0.01, \* < 0.05. . . . . 17

8 Mean CO<sub>2</sub> flux (n=3) and standard deviations per plot treatment at lower moisture conditions (M1). Compaction with 200 kPa at day 4 indicated with dotted line. Letters indicate statistical significances of pairwise comparisons between treatments and days (p < 0.05). Control A (turquoise) always had a significantly higher CO<sub>2</sub> flux than C (orange). A significant reduction in CO<sub>2</sub> fluxes on days 5-7 compared to days 1-3 shows compaction effect in plot treatment C. Control A showed significantly lower CO<sub>2</sub> fluxes on day 5 comparing to days 1-3 and no difference between days 1, 2, 6 and 7. . . . . 18

9 Mean CO<sub>2</sub> flux (n=3) and standard deviations per plot treatment at higher moisture conditions (M2). Compaction with 200 kPa at day 4 indicated by dotted line. Letters indicate statistical significances of pairwise comparisons between treatments and days (p < 0.05). Control A (turquoise) had significantly higher CO<sub>2</sub> fluxes than C (orange) except at day 6. Significant reduction in CO<sub>2</sub> fluxes on days 5-7 compared to days 1-3 show compaction effect for both plot treatments. Treatment C had significantly lower CO<sub>2</sub> flux on day 7 compared to previous days. . . . . 18

10 Differences in mean CO<sub>2</sub> fluxes and standard deviations (n=3) at moist soil conditions (M1) per pressure level (100, 200, 300 kPa) after compaction (Days 5-7). Plot treatment A and C show similar pattern, thus only C is represented in this figure. Letters indicate statistical significances of pairwise comparisons between pressures per day (p < 0.05). Significant differences between CO<sub>2</sub> fluxes compacted with 100 and 300 kPa were found on day 6 and 7. . . . . 20

- 11 Differences in mean CO<sub>2</sub> fluxes and standard deviations (n=3) at higher moisture conditions (M2) per pressure level (100, 200, 300 kPa) after compaction (Days 5-7). Plot treatment A and C show similar pattern, therefore only C is represented in this figure. Letters indicate statistical significances of pairwise comparisons between pressures per day ( $p < 0.05$ ). Significant differences between CO<sub>2</sub> fluxes compacted with 100 and 200 kPa were found on all days and 100 and 300 kPa on day 7. . . . . 20
- 12 Example of a typical dynamic in CO<sub>2</sub> concentration [ppm] before, during and after compaction measured in the head-space connected to compression machine. Grey bars indicate the start and end point of the compaction. . . . . 22
- 13 Differences in mean CO<sub>2</sub> fluxes and standard deviations (n=3) directly before and after compaction with 200 kPa per moisture level (M1, M2) and plot treatment (A, C). Significant reduction in CO<sub>2</sub> emissions after compaction ( $p < 0.0001$ ). Control A had significant higher CO<sub>2</sub> fluxes than C ( $p = 0.0014$ ) and differences between moisture content ( $p = 0.0001$ ). Significant p-values of ANOVA using a linear mixed effect (lme) model: \*\*\*  $< 0.001$ , \*\*  $< 0.01$ , \*  $< 0.05$ . . . . . 22
- 14 Differences in mean initial porosity at 1 kPa (n=9) and mean porosity after compaction (n=3) and standard deviations per moisture level (M1, M2) and pressure level (100, 200, 300 kPa). Letters indicate statistical significances of pairwise comparison between plot treatment (A, C) and pressures ( $p < 0.05$ ). Control A (turquoise) had significant higher porosity than C (orange) ( $p = 0.0016$ ) and compaction led to significantly lower porosity ( $p < 0.0001$ ). . . . . 23
- 15 Differences in mean initial WFPS (water filled pore space) at 1 kPa (n=9) and mean WFPS after compaction (n=3) and standard deviations per moisture level (M1, M2) and pressure level (100, 200, 300 kPa). The triangle marks a potential outlier. Letters indicate statistical significances of pairwise comparison between plot treatment (A, C) and pressures ( $p < 0.05$ ). Higher mechanical loading led to higher WFPS ( $p < 0.0001$ ). No difference between plot treatment was found. . . . . 23
- 16 Example of the measured applied stress during compaction over time. After the target pressure (here 200 kPa) was reached the piston stayed in that position for 120 seconds without applying further vertical stress on the soil core. . . . . 24

- 17 Example of a measured compression curve as a function of void ratio ( $e$ ) and the logarithm of applied stress ( $\sigma$ ) for plot treatment A (upper curve) and C (lower curve). Grey points indicate the measured values while the red and blue line, respectively express the virgin compression line (VCL) and swelling line (SL). The slopes of the virgin compression line and swelling line are termed  $C_c$  and  $C_s$ . Both indices  $C_c$  and  $C_s$  were larger for A than C ( $p < 0.0001$ ), indicating lower compressibility and rebound for peat soils with sand addition. 25
- S1 Dynamics of  $\text{CO}_2$  concentration [ppm] without compaction measured in head-space connected to the compression machine,  $R^2 = 0.99$ ,  $p < 0.0001$ . . . . . 32
- S2 Mean specific  $\text{CO}_2$  flux ( $n=3$ ) and standard deviations per plot treatment at lower moisture conditions (M1). Compaction with 200 kPa at day 4 indicated with dotted line. Letters indicate statistical significances of pairwise comparisons between treatments and days ( $p < 0.05$ ). Specific  $\text{CO}_2$  flux was calculated by normalizing gas flux with corresponding  $C_{org}$  content of dry soil weight. Thereby, no significant difference between specific  $\text{CO}_2$  flux of control (A, orange) and samples with sand addition (C, turquoise) was found. . . . . 34
- S3 Mean specific  $\text{CO}_2$  flux ( $n=3$ ) and standard deviations per plot treatment at lower moisture conditions (M2). Compaction with 200 kPa at day 4 indicated with dotted line. Letters indicate statistical significances of pairwise comparisons between treatments and days ( $p < 0.05$ ). Specific  $\text{CO}_2$  flux was calculated by normalizing gas flux with corresponding  $C_{org}$  content of dry soil weight. Thereby, no significant difference between specific  $\text{CO}_2$  flux of control (A, orange) and samples with sand addition (C, turquoise) was found. . . . . 34
- S4 Differences in mean initial air-filled pore space (AFPS = porosity-VWC) at 1 kPa ( $n=9$ ) and mean AFPS after compaction ( $n=3$ ) as well as standard deviations per moisture level (M1, M2) and pressure level (100, 200, 300 kPa). The triangle marks a potential outlier. Letters indicate statistical significances of pairwise comparison between plot treatment (A, C) and pressures ( $p < 0.05$ ). Linear mixed-effect model of ANOVA included factors plot treatment and interaction of pressure and moisture level. Higher mechanical loading led to higher AFPS ( $p < 0.0001$ ). No difference between plot treatment was found. . . . . 35

## List of Tables

1	Soil properties of the topsoil (0-10 cm) for both plot treatments A (control) and C (sand addition). Standard deviations in brackets and significant differences between plot treatments indicated according to p-values of Wilcoxon rank sum test: *** < 0.001, ** < 0.01, * < 0.05. <sup>1</sup> (Berglund 2011), <sup>2</sup> initial values before compaction. . . . .	7
2	Mean VWC (volumetric water content) and WFPS (water-filled pore space) and standard deviations in brackets for both plot treatments (A and C). "M1" samples were air-dried at 30 °C for 24 h and "M2" represents field fresh samples. P-values of Wilcoxon rank sum test indicate significant differences between plot treatment: *** < 0.001, ** < 0.01, * < 0.05. . . . .	9
3	Significant treatment effects and interactions on CO <sub>2</sub> emissions of the incubator measurement. ANOVA conducted using a linear-mixed effect (lme) model with cylinder and plot number as random effects and a time series structure. Significant p-values: *** < 0.001, ** < 0.01, * < 0.05. . . . .	17
4	Compression and recompression index C <sub>c</sub> and C <sub>s</sub> per plot treatment A and C. Significant differences between plot treatment indicated with significant level. P-values of Kruskal Wallis test: *** < 0.001, ** < 0.01, * < 0.05. . . . .	25
S1	Significant treatment effect of soil compaction indicated by p-values of ANOVA with linear mixed effect (lme) model between measured days per plot treatment (A, C), moisture level (M1, M2) and pressure level (100, 200 and 300 kPa). Significant p-values: *** < 0.001, ** < 0.01, * < 0.05 and n.s > 0.05. . . . .	33

## List of Abbreviations

AFPS	Air-filled pore space
ANOVA	Analysis of variance
$C_c$	Compression index
CH <sub>4</sub>	Methane
CO <sub>2</sub>	Carbon dioxide
$C_{org}$	Organic carbon
$C_s$	Recompression/ Swelling index
$C_{total}$	Total carbon
$e$	Void ratio
GHG	Greenhouse gas
lme model	Linear mixed-effect model
$n$	Sample size
N <sub>2</sub> O	Nitrous oxide
$N_{total}$	Total nitrogen
$\sigma$	Vertical stress
SL	Swelling line
VCL	Virgin compression line
VWC	Volumetric water content
WFPS	Water-filled pore space

## 1 Introduction

Peatlands store about 1/3 of global soil carbon while covering only 3 % of the earth's surface (Joosten and Clarke 2002; Page and Baird 2016). They have a thick layer of organic material and typically organic matter contents above 30 % (dry weight), accumulated over centuries or millennia (FAO 2014; Page and Baird 2016). The majority is located in the northern hemisphere in temperate lowlands and montane areas (FAO 2014). Peatlands are distinguished between nutrient-rich fens and nutrient-poor bogs, depending on the water source and nutrient inflow (Page and Baird 2016). The formation of peatlands is always ongoing when the input of carbon to the ecosystem is higher than the outflow (Page and Baird 2016). Mineralization of the organic material is usually slow due to anaerobic conditions and at low temperatures. Peat soils are very porous and have low bulk density, so they have high water-holding capacities (Page and Baird 2016). Many natural peatlands were drained, limed and fertilized for cultivation (Joosten and Clarke 2002). This leads to fast oxidation and degradation of the organic matter. Therefore, natural peatlands act as a net carbon sink while cultivation leads to high GHG emissions (Page and Baird 2016). Agriculture and forestry, the most widespread use of peat soils, are the main driver for CO<sub>2</sub> and N<sub>2</sub>O emissions (K. Berglund 1996; Joosten and Clarke 2002; Page and Baird 2016; Lennartz and Liu 2019). For Sweden, it is estimated that 6-8 % of the annual anthropogenic GHG emissions arise from cultivated organic soils (Ö. Berglund and K. Berglund 2011). In order to propose mitigation measures to reduce the impact of peat soils to climate change, the influence of different agricultural practises such as soil compaction and sand addition on GHG fluxes has to be determined.

Soil compaction is problematic for agricultural purposes as it negatively affects soil structure and crop growth (Keller et al. 2012; Stolte et al. 2015). However, there have been some contradictory studies showing that compaction of cultivated organic soils enhances crop yield (Othman et al. 2009; Reichert et al. 2009; Melling 2016). Mechanical loading increases the bulk density, improves anchorage of roots and nutrient supply while fertilizer leaching is reduced (Busman et al. 2021). The reduction of air-filled pore space and changes in water flow influences microbial activity and mineralization rate (Beare et al. 2009; Stolte et al. 2015). Thus, it can be expected that compaction reduces CO<sub>2</sub> emission. On the other hand, Busman et al. (2021) observed that compacted peat soils have higher CO<sub>2</sub> emission than uncompacted peat soils. These findings are contradictory to those studies conducted for cultivated mineral soils, showing a reduction in GHG emissions after compaction (Teepe et al. 2004; Ruser et al. 2006; Gregory et al. 2007; Frey et al. 2009; Weisskopf et al. 2010; Mordhorst et al. 2014). Information on the effect of compaction on cultivated peat soils and its influence on carbon and nitrogen cycle is very

scarce. Therefore, the objective of this study is to investigate the effect of compaction with different mechanical loadings on GHG emissions of peat soils.

## **1.1 GHG emission of peat soils**

GHG emissions of peat soils are dependent on climate, microbial activity, intrinsic soil properties such as peat type, substrate quality, oxygen supply and water content as well as land use management (K. Berglund 1996). CO<sub>2</sub> emission derive from aerobic, microbial mineralization of soil organic matter or plant and root respiration (Ryan and Law 2005; Mäkilä and Goslar 2008). In general, increase of soil temperature and optimal moisture conditions for soil respiration lead to higher CO<sub>2</sub> fluxes. Therefore, highest CO<sub>2</sub> emissions of peat soils can be expected during summer, when temperature is high and at medium water content (Ö. Berglund 2011). The transport of CH<sub>4</sub> is either diffuse, plant mediated or by gas bubbles (ebullition) (Bridgham et al. 2013). Methane forms during anaerobic metabolism of microorganism and is highly dependent on soil temperature, soil moisture and compaction (Murdiyarso et al. 2010). Drainage decreases net CH<sub>4</sub> emissions while peat soil compaction enhances production of CH<sub>4</sub> due to altered aeration in the soil matrix (Murdiyarso et al. 2010; Nawaz et al. 2013). In spring and autumn, peaking N<sub>2</sub>O emissions can be observed (Ö. Berglund 2011) because of an increased mineralization rate due to drying and rewetting (DeLuca et al. 1992; Tiemeyer et al. 2016). Nitrous oxide forms during nitrification and denitrification (Firestone and Davidson 1989). At high water contents, denitrification is the most important process leading to very high N<sub>2</sub>O emissions from peat soils (Pihlatie et al. 2004; Ruser et al. 2006; Ö. Berglund 2011).

## **1.2 Influence of sand addition on GHG emission**

Peat soils usually have a low bearing capacity, low bulk density and high porosity. In agricultural management, this has to be considered because it increases the risk of vehicles sinking in the peat (Uusitalo and Ala-Illomäki 2013). This is a limiting factor for cultivation, especially for sowing in early spring. Therefore, sand addition is a commonly used tool to improve soil properties and trafficability for agricultural use (McCoy 1998; Walczak et al. 2002; Sognnes et al. 2006; Ö. Berglund 2020). Increased mineral content leads to higher bulk density, and changes in hydraulic conditions enhance soil stability (Sognnes et al. 2006). Furthermore, incorporation of sand into cultivated peat soils can reduce rapid degradation of organic matter and improve physical properties for plant growth (McCoy 1998; Walczak et al. 2002; Sognnes et al. 2006; Ö. Berglund 2020). Changes in porosity and aeration might alter GHG exchange, resulting in

lower CO<sub>2</sub> emissions when mineral content is increased (Ö. Berglund 2020). The main driver for altered GHG emissions might be the reduction of soil water contents induced by sand addition (Mattsson 2018). In an ongoing field trial, Ö. Berglund (2020) investigates GHG emissions on peat with sand additions and observed trends in lower CO<sub>2</sub> emissions and increased bearing capacity. This study is part of that project and encompasses lab and field GHG measurements to support these findings.

### **1.3 Influence of soil compaction on GHG emissions**

Soil compaction due to vehicular traffic is a well-known problem in agriculture by affecting soil structure and ecosystem functioning. Compaction is defined as densification and distortion of soil when applied stresses exceed soil strength (Huber et al. 2008). The densification leads to a reduction of total and air-filled porosity, leading to altered aeration and water flow. This might change microbial respiration, nutrient cycling, gas flow and hence GHG emissions (Stolte et al. 2015). For mineral soils, several studies have shown that the reduction of aeration by soil compaction induces a significant increase of N<sub>2</sub>O emissions by denitrifying microorganisms (Teepe et al. 2004; Ball et al. 2008). The reduction of macropore volume and increase in water-filled pore space (WFPS) in forest soils leads up to 40 % higher N<sub>2</sub>O emissions and up to 90 % decrease of CH<sub>4</sub> consumption (Teepe et al. 2004). Accordingly, soils can turn from being a CH<sub>4</sub> sink to a source by compaction which has been shown for agricultural, mineral soils (Ruser et al. 1998; Sitaula et al. 2000). Mordhorst et al. (2014) observed a short-time burst effect of CO<sub>2</sub> due to outgassing of compressed pores during compaction for Luvisols. Comparing the day before and after compaction they found significantly lower CO<sub>2</sub> emissions due to decreased soil respiration (Mordhorst et al. 2014). This biological effect is also dependent on the intensity of compaction where higher mechanical stress leads to lower CO<sub>2</sub> respiration (Frey et al. 2009). Furthermore, the effect of CO<sub>2</sub> reduction after compaction can be dependent on water content and soil texture (Gregory et al. 2007; Weisskopf et al. 2010). However, these studies were conducted with mineral soils. Thus, it is unclear whether these findings are applicable for organic soils. Contradictory, a recent study measured higher CO<sub>2</sub> emissions and lower CH<sub>4</sub> emissions at higher bulk densities due to packing for peat soils (Busman et al. 2021). In consequence, more studies are needed to assess GHG emissions from compacted organic soils.

### **1.4 Compressive behaviour of peat soils**

Peat soils are known for their problematic conditions for engineering purposes and agricultural management. In general, peat soils have a high porosity, high void ratio, low bulk density and low bearing capacity.

These conditions explain the low soil strength, although the compressive behaviour of peat soils is complex. Peat soils are very heterogeneous both laterally and vertically due to different stages of degradation, plant residue and vegetation (Den Haan 1997). The compressibility is dependent on the degree of decomposition and peat type (Asselen et al. 2009; Yang et al. 2016; Canakci et al. 2019). Therefore, it is possible to have high variability in bearing capacity within and between stands (Uusitalo and Ala-Ilomäki 2013). However, the bearing capacity and soil strength determine the feasibility of heavy machinery traffic in these areas. This variability has to be taken into account for the predictions of mechanical behaviour, as soil mechanical properties are dependent on the intrinsic properties of soil.

Many studies, analyzing mechanical behaviour of peat soils, are conducted for engineering purposes. There the focus lies on long-term settlement behaviour, secondary and tertiary compression of peat soils (Ajlouni 2000). For that reason, compaction stresses are applied in increment loading tests, where every loading step lasts for 24 hours or multiple days (Rahman et al. 2004; Wong et al. 2009; Yang et al. 2016; Canakci et al. 2019). Vehicular traffic on cultivated peat soils is little studied and results of long-term compaction trials might not be applicable to describe mechanical behaviour of peat soils to short-term compaction. Vennik et al. (2019) used a loading time of 90 seconds for the vertical stress of 100 kPa, which is still two magnitudes higher than the normal passage of a tyre. The approximate applied stress by an agricultural tyre at 5 km/h lasts for 2 seconds while the loading with  $> 0.5$  of maximum stress affects the soil only 1 second (Keller et al. 2012). Therefore, compaction studies with shorter loading and holding times are needed to simulate vehicular traffic.

Resistance to compression (soil strength) is negatively affected by higher soil organic carbon contents. However, soils with higher soil organic carbon contents are more resilient to compaction (Zhang et al. 2005; Kuan et al. 2007; Keller et al. 2011). Soil resistance to compaction is commonly expressed by the compression index  $C_c$ , which indicates the soil deformation behaviour when mechanical loading is increased. After compaction, when the load is removed, the soil rebounds. This behaviour is expressed by the recompression index  $C_s$  (Kuan et al. 2007; Keller et al. 2011; ElMouchi et al. 2021). The properties of  $C_c$  and  $C_s$  are typically described by the relationship between the logarithm of applied stress and the void ratio shown in Fig. 1. Thereby,  $C_c$  represents the slope of the virgin compression line (VCL), which follows along the loading path, while  $C_s$  is determined as the slope of the swelling line (SL) (Keller et al. 2011). When the void ratio is high, the particle to particle contact is lower so that less energy is needed to rearrange particles (Keller et al. 2011). Consequently, high initial void ratios of organic soils lead to a large deformation when external load is applied (ElMouchi et al. 2021). This means that soils are less

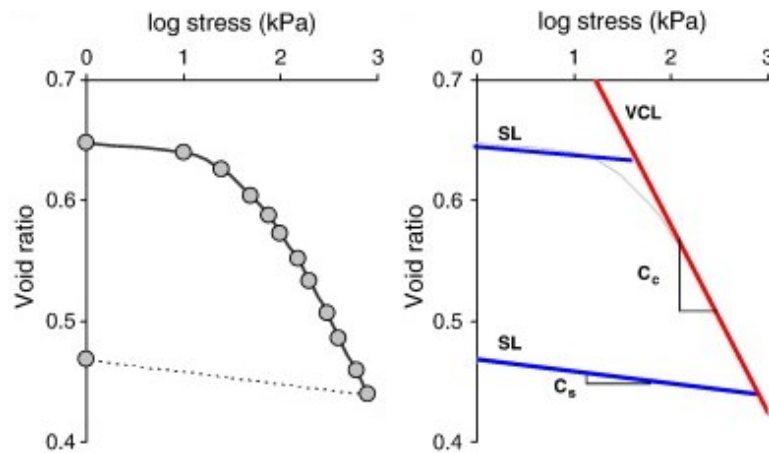


Fig. 1: Left: Measured compression curve described by void ratio ( $e$ ) as a function of the logarithm of applied stress ( $\sigma$ ). Right: Idealised compression behaviour of soil which is plastic and irreversible along the virgin compression line (VCL) and elastic and reversible along the swelling line (SL). Slopes of VCL and SL are termed compression index  $C_c$  and recompression index  $C_s$  (Keller et al. 2011).

resistant to compaction (high  $C_c$ ) at high initial void ratio. Organic soils have  $C_c$  ranging between 0.5-18, while clay soils are lower and lie between 0.2-0.8 (Lefebvre et al. 1984; Yamaguchi et al. 1985; Ajlouni 2000; Abdel Kadar 2010; EIMouchi et al. 2021). High water contents of organic soils and initial void ratio explain the relatively high  $C_c$  of organic soils (EIMouchi et al. 2021). The rebound index  $C_s$  is positively correlated to organic content and precompression stress (Lefebvre et al. 1984; Yamaguchi et al. 1985). However, the rebound behaviour of peat soils is very complex and further studies on  $C_s$  are missing.

In this study, organic soils with and without sand addition were compacted with different vertical stresses to analyse the mechanical behaviour and (re-)compression characteristics. Sand addition leads to stabilization of the peat soil by reducing void ratio, porosity and increasing bulk density (Sognnes et al. 2006). Therefore, peat soils with sand addition should be more resistant to compaction and have lower  $C_c$ . Furthermore, water content and different stress intensities might have an influence on  $C_c$  and  $C_s$ .

## 1.5 Hypotheses

This report is divided into two parts, whereas the first encompasses field and laboratory GHG measurements as well as the determination of chemical and physical properties of the studied peat soil. The second part contains the development of the compaction tests with in-situ GHG emission measurements and the description of some mechanical properties of peat soil. Thereby, following hypotheses will be examined:

- Sand addition reduces CO<sub>2</sub> emissions
- CO<sub>2</sub> emissions are lower after compaction due to decrease in soil respiration
- N<sub>2</sub>O emissions are higher after compaction due to reduction in aeration in the soil matrix
- An increase in mechanical loading has a higher effect on GHG fluxes
- An increase in mechanical loading leads to a higher change in porosity and WFPS
- C<sub>c</sub> and C<sub>s</sub> of organic soils are lower with sand addition
- C<sub>c</sub> and C<sub>s</sub> are dependent on soil physical parameters (organic matter content, initial water content, initial void ratio and initial porosity).

## 2 Material & Methods

Field and laboratory measurements of undisturbed soil samples with and without sand addition were conducted to evaluate the influence of sand addition on GHG emissions. After three days of GHG flux measurements in an incubator, samples were compacted with a uniaxial compression machine with vertical stresses of 100, 200 or 300 kPa to simulate realistic contact pressures of tractors (Arvidsson and Keller 2007; Ungureanu et al. 2016). A new method to measure the dynamics of GHG during compaction as well as directly before and after was developed by connecting the gas analyzer via tubes to the compression machine. This method provides the opportunity to investigate direct changes in GHG concentrations during and shortly after compaction, while the incubator measurements investigate the change in GHG emissions three consecutive days before and after compaction. Upon completion of the compaction and GHG measurements, soil samples were extracted and further processed for soil chemical and physical analysis. Afterwards, calculations of the mechanical behaviour of the soil to describe the compressibility and of peat soils with and without sand addition were conducted. In this report, vertical stress and (compaction) pressure were used as synonyms to improve read-flow, although vertical stress is the correct, scientific expression to describe the compaction of soils.

### 2.1 Field design and field site description

The field site is located in Broddbo at the peatland area Bälänge mossar (60.03N, 17.43E) and vegetated with timothy (*Phleum pratense*). Since 2016, there is an ongoing field trial with different amounts of

sand additions in a randomized block design (Fig. 2). There are three blocks with each a control plot (A), a plot with 2.5 cm (B) and one with 5 cm foundry sand (C) mixed into 10-15 cm depth of the topsoil, respectively. The field is fertilized twice a year (spring, autumn) and harvested in the beginning of July as well as in the beginning of September. The field site classifies as a fen peat with a von Post degradation degree of H9-H10 (Ö. Berglund 2011) and  $C_{org}$  and  $C_{total}$  contents are very similar, which is typical for peat soils. A summary of the mean values of the chemical and physical properties for plot treatment A and C measured 2021 are presented in table 1, whereas the methodology is explained in section 2.7. The results align with measurements conducted in 2017 (Mattsson 2018; Ö. Berglund 2020). Incorporation of sand leads to changes in the soil composition. The organic matter content is three times lower with sand addition and there are differences between  $C_{org}$ ,  $C_{total}$  and  $N_{total}$  contents between plot treatments. Furthermore, bulk density and particle density are higher, whereas the initial porosity is lower when sand is added.

Table 1: Soil properties of the topsoil (0-10 cm) for both plot treatments A (control) and C (sand addition). Standard deviations in brackets and significant differences between plot treatments indicated according to p-values of Wilcoxon rank sum test: \*\*\* < 0.001, \*\* < 0.01, \* < 0.05. <sup>1</sup>(Berglund 2011), <sup>2</sup>initial values before compaction.

Parameters	Treatment A	Treatment C	Significance level
von Post	H9-H10 fen peat <sup>1</sup>	H9-H10 fen peat <sup>1</sup>	
pH (H <sub>2</sub> O)	6.15 (± 0.05)	6.46 (± 0.11)	**
Organic matter [%]	82.06 (± 5.88)	26.35 (± 6.13)	***
$N_{total}$ [%]	3.32 (± 0.22)	0.77 (± 0.26)	***
$C_{total}$ [%]	47.42 (± 2.36)	12.78 (± 3.56)	***
$C_{org}$ [%]	47.11 (± 2.33)	12.46 (± 3.53)	***
Particle density [g cm <sup>-3</sup> ]	1.63 (± 0.05)	2.25 (± 0.10)	***
Bulk density [g cm <sup>-3</sup> ] <sup>2</sup>	0.30 (± 0.02)	0.67 (± 0.12)	***
Porosity [%] <sup>2</sup>	81.92 (± 0.86)	70.14 (± 4.57)	***

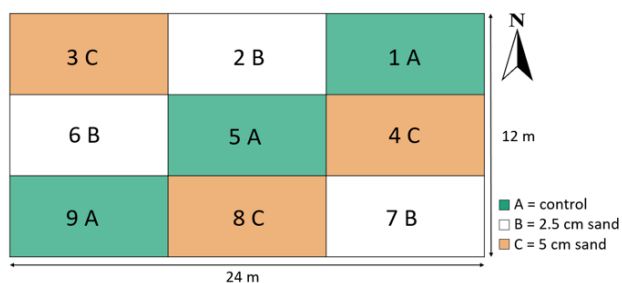


Fig. 2: Left: The field experiment at Brodöbo has a randomized block design with different amounts of sand additions. A represents the control plot (turquoise), B 2.5 cm foundry sand (white) and C 5 cm foundry sand (orange) mixed into 10-15 cm topsoil. Each plot is 8 m by 4 m and is vegetated with timothy (*Phleum pratense*). Right: GHG flux measurement with manual opaque chamber and Gaset GT5000 Terra portable gas analyzer. (Photo: Antonia Hartmann).

## 2.2 Field measurements

Field GHG measurements (CO<sub>2</sub>, CH<sub>4</sub>, N<sub>2</sub>O) were conducted six times between 19<sup>th</sup> April and 14<sup>th</sup> July 2021 using a Gaset GT5000 Terra portable gas analyzer and at the first date Vaisala MI70 CO<sub>2</sub>-meter (Fig. 2). Permanent polyvinylchloride frames (inner diameter 18.0 cm) were installed on each plot. For the measurements, a manual opaque chamber (inner diameter 18.0 cm and 18.0 cm height) was attached to the frames (Jordan 2016). The measuring time was 5 minutes and the sampling rate every 5 and 15 seconds for Gaset and Vaisala device, respectively. The emission rate in the chamber headspace was calculated using the ideal gas law and linear regression. The gas flux *F* over the closing time was estimated in mg m<sup>-2</sup> h<sup>-1</sup> for CO<sub>2</sub> and μg m<sup>-2</sup> h<sup>-1</sup> for CH<sub>4</sub> and N<sub>2</sub>O with equation 1. Thereby, only rates with a linearity of R<sup>2</sup> ≥ 0.85 for CO<sub>2</sub>, N<sub>2</sub>O and ≥ 0.60 for CH<sub>4</sub> were considered (Norberg 2017). The first 30 seconds of the measurements were rejected to account for non-linear fluxes occurring directly after closure of the chamber.

$$F = \frac{\frac{\Delta c}{\Delta t} * V}{R * T} * p * m \quad (1)$$

Where Δ*c* is the average change in gas concentration during measuring time Δ*t* (ppm time<sup>-1</sup>), *V* is the volume of the chamber and tubes (m<sup>3</sup>), *A* the base area of the chamber (m<sup>2</sup>), *p* the atmospheric (Pa), *m* the molecular mass of CO<sub>2</sub> (44.01 g mol<sup>-1</sup>), *R* the ideal gas constant (8.3145 J mol<sup>-1</sup> K<sup>-1</sup>) and *T* the air temperature (K). The average height of the PVC frames was estimated with a ruler at four points and included in the headspace volume. Furthermore, the volumetric water content (VWC) and soil temperature were determined with a WET sensor (HH2 moisture meter, DELTA-T Devices, Cambridge, England) at three points next to the frames to avoid disturbance. Air temperature was measured using the temperature sensor attached to the opaque chamber.

In the statistical analysis only treatment A and C were compared, as treatment B was not included in the laboratory experiment. A linear regression analysis was used to check the analysis of variance (ANOVA) prerequisites of a linear relationship between measured soil temperature and VWC to the response variable. Different linear mixed-effect (lme) models with a time series structure and plot number as random effect were conducted to analyze potential treatment effects and interactions between plot treatment (A, C), soil temperature and VWC. The CO<sub>2</sub> fluxes were log-transformed to improve the residuals of the model. The best model included temperature and plot treatment without VWC and any interactions and was used in the ANOVA. Fluxes of CH<sub>4</sub> and N<sub>2</sub>O were below detection limit, and hence excluded in the analysis.

Statistical analysis was carried out in RStudio 4.0.0 (R Core Team 2020) using the package “nlme” for the model (Pinheiro et al. 2020).

### 2.3 Soil sampling and preparation

In spring 2021, undisturbed cylindrical soil cores (height 10 cm, diameter 7 cm) were sampled at each plot of the control treatment (A) and 5 cm foundry sand (C) with six replicates leading to 36 samples. The soil samples were very moist and had a high variance in water contents. High water contents are problematic for the compaction experiment due to methodological reasons discussed in section 4.5. Consequently, the water content of half of the samples was reduced by air-drying them at 30 °C for 24 h. Mean VWC and water-filled pore space (WFPS) and standard deviations per plot treatment are shown for “air-dried” and fresh samples, which thereafter are called “M1” and “M2”. The factor variable of “M1” and “M2” samples will be denoted as “moisture level”. Wilcoxon rank sum tests were conducted for analyzing the difference between moisture level of VWC and WFPS per plot treatment.

Table 2: Mean VWC (volumetric water content) and WFPS (water-filled pore space) and standard deviations in brackets for both plot treatments (A and C). “M1” samples were air-dried at 30 °C for 24 h and “M2” represents field fresh samples. P-values of Wilcoxon rank sum test indicate significant differences between plot treatment: \*\*\* < 0.001, \*\* < 0.01, \* < 0.05.

Moisture level	Treatment A		Treatment C	
	VWC [%]	WFPS [%]	VWC [%]	WFPS [%]
M1	62.2 (± 2.9)	76.4 (± 4.4)	52.8 (± 3.3)	74.2 (± 3.4)
M2	70.3 (± 1.9)	85.4 (± 2.2)	55.8 (± 6.1)	81.0 (± 8.4)
Significance level	***	***	**	**

### 2.4 Description of the compaction experiment

In this study, soil samples were compacted with 100, 200 or 300 kPa to mimic contact pressures of different vehicles used in agriculture (Arvidsson and Keller 2007; Ungureanu et al. 2016). Compaction trials were conducted in a uniaxial compression machine with two 10 KN load cells (S9M/10 KN, HBM GmbH, Darmstadt, Germany) to apply the vertical compaction force via the piston on the soil core. The piston moves down and compresses the soil in the cylinder with a defined loading rate (0.5 mm/sec) until the targeted vertical stress ( $\sigma$ ) is reached. Then the piston stays in place for 120 seconds. Afterwards, the piston is unloaded to 1 kPa ( $\log(\sigma) = 0$ ) with a rate of 5 mm/sec. These settings were chosen to mimic machinery traffic with different contact pressures and a relative short compression and holding time.

The loading rate and holding time were still two magnitudes higher than at field conditions. This time was chosen to capture GHG dynamics during compaction described in section 2.6 and was similar to the 180 seconds compaction time of Ball et al. (2008). Data of applied stress on soil core and displacement height were measured per second during the whole loading and holding time. After unloading, the final displacement height was measured at four points in the cylinder with a ruler (Fig. 3).

## 2.5 Incubator measurements

Greenhouse gases (CO<sub>2</sub>, CH<sub>4</sub>, N<sub>2</sub>O) were measured on three consecutive days before and after compaction in an air-tight polypropylene jar (height 12 cm, diameter 11 cm) connected to the gas analyzer (Gasmeter GT5000 Terra portable gas analyzer) shown in Fig 3. The measurements took 3.5 to 10 minutes with a sampling rate of 5 seconds until at least a 100 ppm change in CO<sub>2</sub> emissions was detected. The emission rate was calculated with the ideal gas law and the linear change of each gas during closure time while the first 30 seconds after closure were omitted. Furthermore, only measurements with a linearity of  $R^2 \geq 0.85$  for CO<sub>2</sub>, N<sub>2</sub>O and  $\geq 0.60$  for CH<sub>4</sub> were used (Norberg 2017). The gas fluxes  $F$  in mg g<sup>-1</sup> h<sup>-1</sup> were calculated using equation 2, where  $\Delta c/\Delta t$  is the average change in concentration of the gas during measuring time (ppm time<sup>-1</sup>),  $V$  is the volume in the incubator and tubes (m<sup>3</sup>),  $m$  the molecular mass of the gas (g mol<sup>-1</sup>),  $R$  the ideal gas constant (8.3145 J mol<sup>-1</sup> K<sup>-1</sup>),  $T$  the ambient air temperature (K) and  $w$  the dry soil weight (g):

$$F = \frac{\frac{\Delta c}{\Delta t} * V * p * m}{R * T * w} \quad (2)$$

The volume of the incubator was calculated by subtracting the volume of the cylinder from the total volume of the jar and adding the volume of the tubes for in- and outflow to the gas analyzer. Furthermore, the displacement of soil after compaction was measured at four points and included as air volume (Fig 3).

For the statistical analysis, CO<sub>2</sub> and N<sub>2</sub>O emissions were log-transformed to meet normality and homoscedasticity requirements of the four-way-ANOVA. Therefore, only fluxes  $\neq 0$  mg g<sup>-1</sup> h<sup>-1</sup> could be used in the model. Multiple lme models with time series structure, cylinder number and plot as random factors were used to test significances in gas emissions between the different treatments and its interactions: day (days 1-3, 5-7), pressure level (100, 200, 300 kPa), plot treatment (A, C) and soil moisture. The numerical variables, VWC and WFPS did not meet linearity requirements to the response

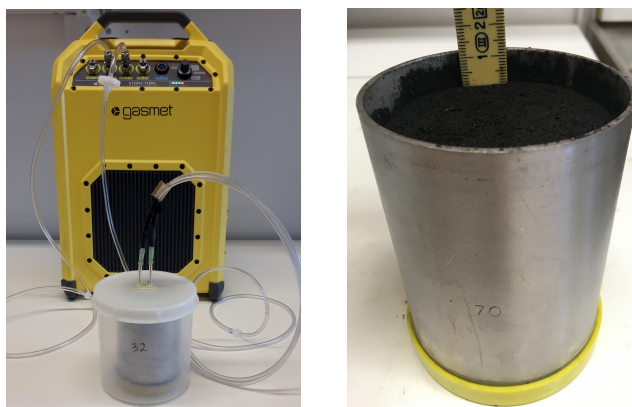


Fig. 3: Left: GHG flux measurements with air-tight polypropylene jar (incubator) and Gaset GT5000 Terra portable gas analyzer Right: Measurement of the displacement height after compaction for exact calculation of the soil physical properties and air volume for GHG flux calculation (Photos: Antonia Hartmann).

variable for the ANOVA, therefore the factor variable “moisture level” (M1, M2) was used as categorical input variable. The best lme model for CO<sub>2</sub> included interactions between day, moisture level and pressure level as well as the interaction of day, moisture level and plot treatment. For N<sub>2</sub>O only differences between days after compaction could be analyzed. The lme model only included the factor day, as many fluxes were not detectable and had to be excluded. Afterwards, ANOVA and post-hoc tests were conducted for pairwise comparisons of least square means for each time point and treatment variables used in the corresponding model. Statistical analysis was carried out in RStudio 4.0.0 (R Core Team 2020) with packages “nlme” (Pinheiro et al. 2020) and “emmeans” (Lenth 2020).

## 2.6 Measurement of GHG dynamics during compaction

In order to capture the GHG dynamics during and shortly before and after compaction, a gas analyzer (Gaset GT5000 Terra portable gas analyzer) was connected via tubes to the compression machine (see Fig. 4). A piston was built to fit the cylinder height of 10 cm and diameter 7 cm. The porous cap ensured gas flow through channels of the piston. To ensure air-tight measurements during the compaction, a rubber (My size 69mm, Singen (Hohentwiel), Germany) was pulled over the cylinder and piston. This method was chosen due to the elasticity and flexibility of the rubber while the sharp edges of the cylinder were covered by a small plastic ring to prevent ripping. The channels were connected to inflow and outflow tubes of the gas analyzer to ensure a circulating system.

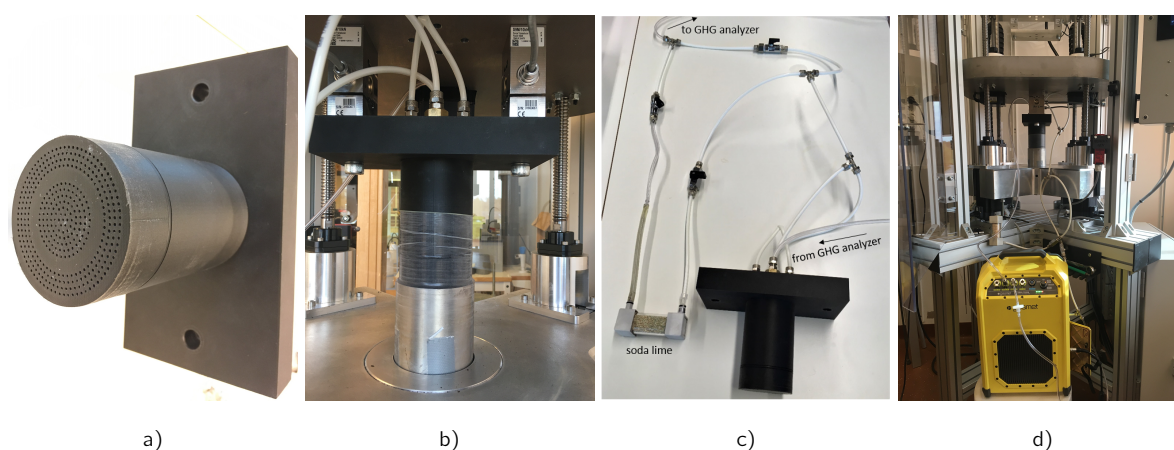


Fig. 4: a) Piston with porous cap and channels through piston core. b) Piston position on soil surface, rubber seals air-tight around piston. c) Tube system connected to piston and integrated valves. Valves on the left side were only open during flushing with soda lime. d) Whole setup of the uniaxial compression machine with a tube connection between piston and GHG analyzer for gas measurements.

Before measuring GHG emissions of soils during compaction, the systems's air-tightness was tested by removing ambient  $\text{CO}_2$ . The system was flushed with soda lime until all ambient  $\text{CO}_2$  was absorbed. Then the connecting valves were closed again, thus the air circulated between an empty cylinder and the GHG analyzer. Over a measuring time of 10 minutes, an increase of 33.3 ppm  $\text{CO}_2$  was detected. This increase is small in comparison to the average change in  $\text{CO}_2$  concentration between start and end of in-situ GHG measurement ( $473.9 \pm 223.2$  ppm). Therefore, leakages of tubes, connectors and rubber could be neglected and the set-up considered as air-tight (Fig 5).

GHG concentrations were measured every second during the compaction as well as 3.5 min directly before and after compaction. The sampling rate of 1 second is the smallest possible for the gas analyzer and chosen to closely observe the dynamics during compaction. The measuring time before and after compaction was selected to have a 100 ppm increase in  $\text{CO}_2$  concentration before and potentially after compaction while not exceeding the detection limit of 2000 ppm  $\text{CO}_2$  and the water vapour limit of the gas analyzer. This was the case in pre-tests due to high microbial activity in peat soils, high water contents and the relatively small volume of the system. Linear emission rates were calculated for fluxes before and after compaction using equation 2. Here,  $V$  included the volume of the tubes as well as the channels in the piston. All  $\text{N}_2\text{O}$  and  $\text{CH}_4$  fluxes were below the detection limit and some  $\text{CO}_2$  fluxes after compaction did not fit the linearity requirements of  $R^2 \geq 0.85$  and had to be excluded.

The statistical analysis to compare  $\text{CO}_2$  fluxes shortly before and after compaction was similar to the incubator experiment described in section 2.5.  $\text{CO}_2$  emissions were log-transformed and an lme model with

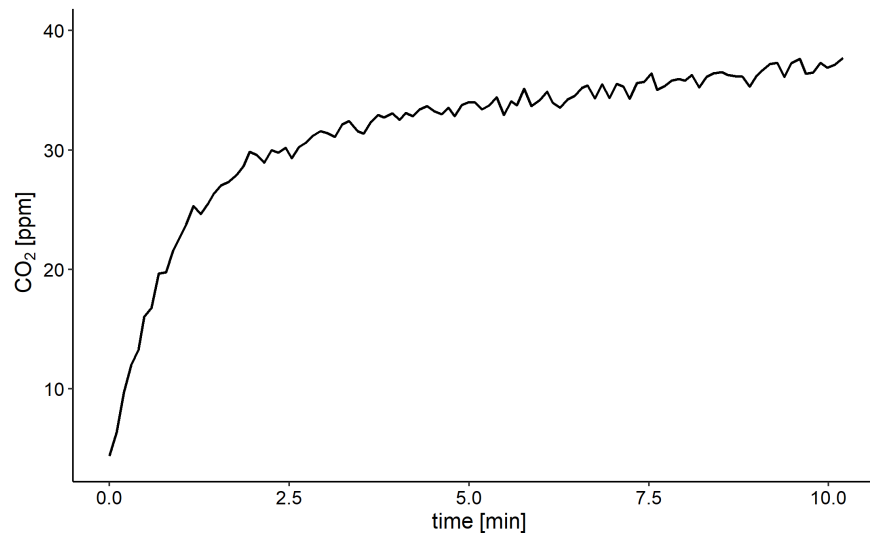


Fig. 5: Increase of CO<sub>2</sub> concentration was 33.3 ppm within 10 minutes after removing ambient CO<sub>2</sub> using soda lime. Therefore, leakage of tubes can be neglected in compaction experiments.

time series structure used to test the influence of the factors time (before, after compaction), pressure level (100, 200, 300 kPa), moisture level (M1, M2), plot treatment (A, C) as well as its interactions. Cylinder and plot number were included as random effects. Moisture level was used as categorical variable, as VWC and WFPS did not meet the model prerequisites. The final model for the ANOVA included factors time, moisture level and plot treatment. Post-hoc tests were conducted for pairwise comparisons for each factor using RStudio 4.0.0 (R Core Team 2020) with the packages “nlme” (Pinheiro et al. 2020) and “emmeans” (Lenth 2020).

## 2.7 Measurement of chemical and physical properties

When the incubator measurements were finished, the soil sample of the cylinder was removed, weighted, homogenized and divided into subsamples for further analysis in order to have exact data of the parameters per cylinder (especially of bulk density, particle density and mineral content). For pH measurements (1:5 deionized water), 5 ml fresh soil was used, shaken for 5 minutes and measured after 30 minutes. A weighted subsample was air-dried for particle density measurement and the rest oven dried at 105 °C for the determination of bulk density, VWC, loss of ignition and C/N analysis. Bulk density calculations [g/cm<sup>3</sup>] were conducted before and after compaction by including the displaced volume for each cylinder. Therefore, a back calculation to get the dry soil weight for the total cylinder was necessary, since only

a weighted subsample could be oven-dried. Organic matter content was determined with the loss of ignition method at 550 °C for 6 h for all 36 cylinders. Soil  $C_{org}$ ,  $C_{total}$  and  $N_{total}$  contents were measured using TruMac CN (LECO, St. Joseph, Michigan). Thereby, only half of the samples were analyzed and compared to literature data. This is a commonly used measure to reduce costs, when high variation within a plot is not expected. Particle density (mass of dry soil/volume of solid soil) was determined by the liquid displacement method, where 10-15 g of air-dried soil (sieved and ground < 2mm) was weighed into a 50 ml flask with two replicates per sample. Then, 35 ml of ethanol (D-sprit 95 %) was added with a digital burette to each flask and magnetically stirred for 20 seconds. The flasks were placed in a water bath at 20 °C. After three days, the flasks were stirred again for several seconds and after a few hours, when the supernatant was clear, ethanol was added until the ring marking. The water content of the air-dried samples at the time of particle density analysis was determined by oven drying at 105 °C overnight and included in the overall calculation:

$$pd = \frac{b * d}{c * (e - f - (0.85 * b))} + \frac{0.85 * b * d}{c} - a \quad (3)$$

where a is the amount of added alcohol [ml], b the weight of air-dried soil in the flask [g], c the weight of air-dried soil sample before oven-drying [g], d the weight of the oven-dried sample [g], e the flask volume (50 ml) and f the magnet volume (0.83 ml).

Based on the parameters, initial and final void ratio (e), porosity ( $\Phi$ ) and WFPS (before and after compaction) were calculated with following formulas:

$$e = \frac{pd}{bd} + \frac{H - h}{h} - 1 \quad (4)$$

where pd is the particle density, bd the bulk density, H the height of cylinder and h the displacement height.

$$\Phi [\%] = \frac{e}{1 + e} * 100 \quad (5)$$

$$WFPS [\%] = \frac{VWC}{n} * 100 \quad (6)$$

Wilcoxon rank sum tests were conducted for comparing physical and chemical soil properties between the plot treatments A and C. Differences in initial porosity and initial WFPS to porosity and WFPS after compaction were analyzed using multiple lme models with cylinder and plot number as random factors and a time series structure in RStudio 4.0.0 (R Core Team 2020) with packages "nlme" (Pinheiro et al. 2020) and "emmeans" (Lenth 2020). The initial model included all factors and interactions: time (before, after compaction), plot treatment, pressure and moisture level. The best fitted model for porosity included time interacting with each pressure level, moisture level and plot treatment. For WFPS, moisture level as well as interactions between pressure and plot treatment with time were combined in the lme model, which was used in the consecutive ANOVA and pairwise comparisons.

## 2.8 Mechanical behaviour of peat soil

The compression curve is expressed by the change of void ratio as a function of the logarithm of applied stress  $\sigma$ . The compression index  $C_c$  was determined as the mean slope of the loading path until the target pressure was reached. In order to take elastic behaviour into account, the slope was calculated between 25 kPa and max. stress ( $\sigma_{max}$ ) (equation 7). The recompression index  $C_s$  was calculated similarly to  $C_c$  as the mean slope of the unloading path from the  $\sigma_{max}$  to 1 kPa (equation 8):

$$C_c = \frac{\Delta e}{\log(\Delta\sigma)} = \frac{e_{25} - e_{max}}{\log(|\sigma_{25} - \sigma_{max}|)} \quad (7)$$

$$C_s = \frac{\Delta e}{\log(\Delta\sigma)} = \frac{e_{final} - e_{max}}{\sigma_{max}} \quad (8)$$

where,  $e_{25}$  is the void ratio at  $\sigma_{25}$  ( $\sigma = 25$  kPa),  $e_{max}$  is the void ratio at  $\sigma_{max}$  and  $e_{final}$  final void ratio after unloading. The relationships between soil compressive indices  $C_c$  and  $C_s$  and other soil properties (organic matter content, initial void ratio  $e$ , initial porosity, initial VWC and initial WFPS) were evaluated by fitting linear regression models. Kruskal wallis test and dunn post hoc test were performed to analyze the effects of plot treatment, moisture level and pressure level on  $C_c$  and  $C_s$ . For this RStudio 4.0.0 (R Core Team 2020) was used with the package "FSA" (Ogle et al. 2021).

## 3 Results

### 3.1 Field measurements

In the field, soils with sand addition (C, orange) had significant lower CO<sub>2</sub> emissions compared to the control samples (A, turquoise,  $p = 0.0431$ ). The change in CO<sub>2</sub> fluxes per treatment, for both soil temperature and VWC during calendar week 16-28 are shown in figures 6 and 7. Each point represents the mean CO<sub>2</sub> flux of the three plots per treatment while the triangle indicates the corresponding soil temperature (VWC). In spring, CO<sub>2</sub> fluxes were lower and raised over the measuring period following the changes in soil temperature ( $p < 0.0001$ ), whereas VWC did not have a significant effect.

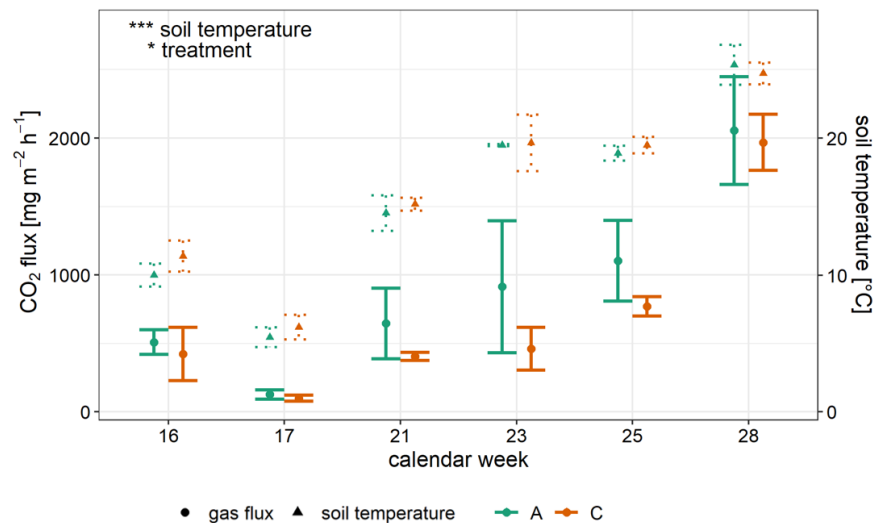


Fig. 6: Mean CO<sub>2</sub> flux and standard deviations of field measurements during calendar week 16-28. Each point represents 3 measuring points per plot treatment. Triangle and dotted bars indicate soil temperature [°C]. CO<sub>2</sub> flux of control A (turquoise) was statistically different from C (orange,  $p = 0.0431$ ). CO<sub>2</sub> fluxes were highly dependent on soil temperature ( $p < 0.0001$ ). Significant p-values of ANOVA using a linear mixed effect (lme) model: \*\*\*  $< 0.001$ , \*\*  $< 0.01$ , \*  $< 0.05$ .

### 3.2 Incubator measurements

The analysis of the incubator measurements shows that all tested factors significantly influenced CO<sub>2</sub> fluxes. Furthermore, significant interactions between the tested variables were found, which are indicated in table 3. Although no correlation between water content and CO<sub>2</sub> emissions was found in the field experiment, the difference in moisture affected the CO<sub>2</sub> emissions in the laboratory experiment. Samples with lower water content (M1) had higher net CO<sub>2</sub> emissions compared to M2 ( $p < 0.0001$ , see figures

8 and 9).

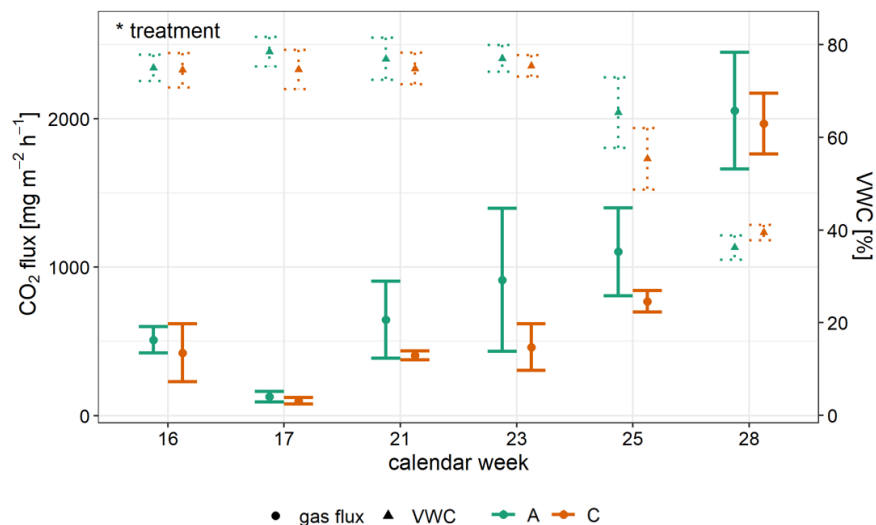


Fig. 7: Mean CO<sub>2</sub> flux and standard deviations of field measurements during calendar week 16-28. Each point represents 3 measuring points per plot treatment. Triangle and dotted bars indicate VWC [%]. CO<sub>2</sub> flux of control A (turquoise) was statistically different from C (orange,  $p = 0.0431$ ). No statistical effect between VWC and CO<sub>2</sub> fluxes was found. Significant p-values of ANOVA using a linear mixed effect (lme) model: \*\*\* < 0.001, \*\* < 0.01, \* < 0.05.

Table 3: Significant treatment effects and interactions on CO<sub>2</sub> emissions of the incubator measurement. ANOVA conducted using a linear-mixed effect (lme) model with cylinder and plot number as random effects and a time series structure. Significant p-values: \*\*\* < 0.001, \*\* < 0.01, \* < 0.05.

Treatment effects on CO <sub>2</sub> fluxes	DF	F-value	p-value	Significance level
day	144	63.805	< 0.0001	***
moisture	25	64.234	< 0.0001	***
pressure	25	3.629	0.0413	*
plot treatment	4	19.974	0.0111	*
<b>Interactions:</b>				
day:moisture	144	14.953	< 0.0001	***
day:pressure	144	5.680	< 0.0001	***
day:moisture:pressure	144	3.117	0.0013	**
day:moisture:plot treatment	144	2.424	0.0383	*

### 3.2.1 Influence of sand addition on CO<sub>2</sub> fluxes

Similar to the field measurement, CO<sub>2</sub> emissions were lower for plot treatment C ( $p = 0.0111$ ) while this effect was dependent on moisture level and measured day ( $p = 0.0383$ ). Figures 8 and 9 show differences in plot treatment per day in combination with significant differences between the measured days. Each

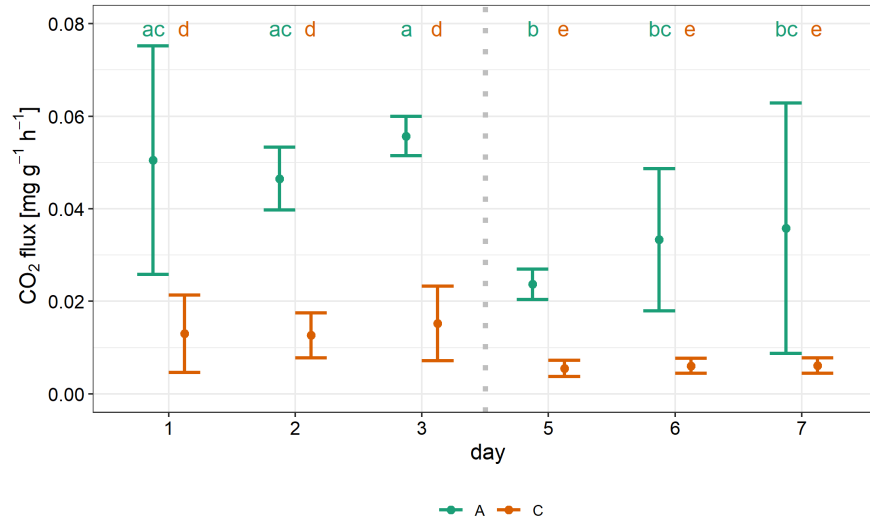


Fig. 8: Mean CO<sub>2</sub> flux (n=3) and standard deviations per plot treatment at lower moisture conditions (M1). Compaction with 200 kPa at day 4 indicated with dotted line. Letters indicate statistical significances of pairwise comparisons between treatments and days ( $p < 0.05$ ). Control A (turquoise) always had a significantly higher CO<sub>2</sub> flux than C (orange). A significant reduction in CO<sub>2</sub> fluxes on days 5-7 compared to days 1-3 shows compaction effect in plot treatment C. Control A showed significantly lower CO<sub>2</sub> fluxes on day 5 comparing to days 1-3 and no difference between days 1, 2, 6 and 7.

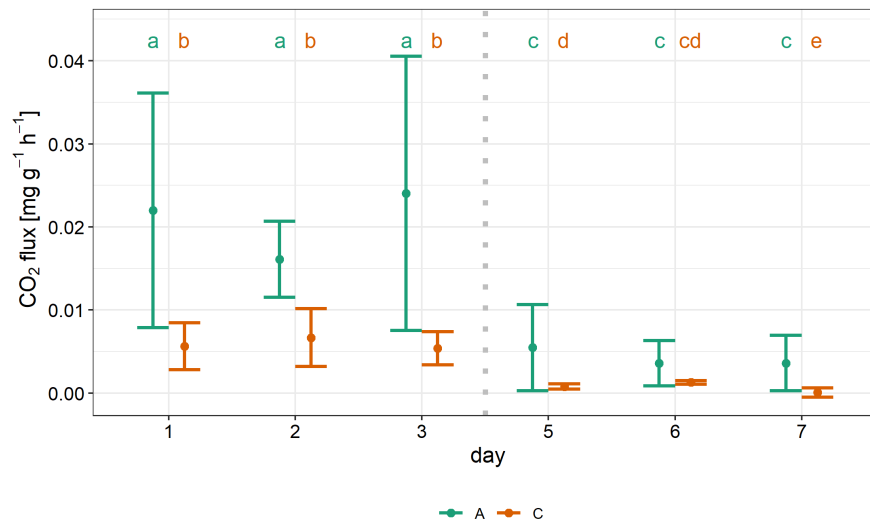


Fig. 9: Mean CO<sub>2</sub> flux (n=3) and standard deviations per plot treatment at higher moisture conditions (M2). Compaction with 200 kPa at day 4 indicated by dotted line. Letters indicate statistical significances of pairwise comparisons between treatments and days ( $p < 0.05$ ). Control A (turquoise) had significantly higher CO<sub>2</sub> fluxes than C (orange) except at day 6. Significant reduction in CO<sub>2</sub> fluxes on days 5-7 compared to days 1-3 show compaction effect for both plot treatments. Treatment C had significantly lower CO<sub>2</sub> flux on day 7 compared to previous days.

point represents three cylinders compacted with 200 kPa on the fourth day at moisture level M1 (Fig. 8) and M2 (Fig. 9). Statistical significances between plot treatments and days are indicated with letters ( $p < 0.05$ ). Both figures show that the control samples A (turquoise) had significantly higher CO<sub>2</sub> fluxes than C (orange). This effect was observed every day, except for samples of M2 on the sixth day, where only a trend was observed ( $p = 0.065$ ).

### **3.2.2 Influence of soil compaction on CO<sub>2</sub> fluxes**

Next to sand addition, CO<sub>2</sub> fluxes were dependent on the day, hence the compaction. In many cases for different moisture levels and pressures, significances between days 1, 2, 3 to 5, 6, 7 were found, showing a large reduction in CO<sub>2</sub> emissions after compaction (see figures 8, 9 and table S1 for compaction pressures 100 and 300 kPa). At lower moisture conditions (M1), a compaction effect at a mechanical loading of 200 kPa was measurable for treatment C while the pattern for treatment A was more unclear (Fig. 8). For treatment A when days 1-3 and 5 are compared, a compaction effect was detected. However, no significant change in CO<sub>2</sub> fluxes comparing days 1 and 2 to 6 and 7 was found. Furthermore, no compaction effect on CO<sub>2</sub> fluxes was measured for M1 with a mechanical loading of 100 kPa for both plot treatments. At higher water contents (M2), CO<sub>2</sub> fluxes were significantly lower after compaction (days 5-7) compared to pre-compaction fluxes (day 1-3, Fig. 9). Furthermore, a significant reduction of CO<sub>2</sub> emissions at the seventh day compared to the fifth and sixth days was detected for pressure level 200 kPa.

### **3.2.3 Influence of different mechanical loading on CO<sub>2</sub> fluxes**

The effect of compaction on CO<sub>2</sub> fluxes was dependent on the mechanical loading ( $p = 0.0413$ ) which interacted with moisture level and day ( $p = 0.0383$ ). Before compaction (days 1-3), there was no difference in CO<sub>2</sub> fluxes between the pressure levels. After compaction at days 5-7, differences between some pressures could be observed. Figures 10 and 11 show the mean CO<sub>2</sub> fluxes of plot treatment C at both moisture levels. Each point represents three cylinders and statistical significances between pressures are indicated with letters ( $p < 0.05$ ). Both plot treatments had a similar pattern of differences between pressures. Therefore, only treatment C is shown in both figures. At moisture level M1, only significant differences between mechanical loading of 100 and 300 kPa at day 6 and 7 were found (Fig. 10), indicating lower CO<sub>2</sub> net fluxes at higher compaction pressure. At very moist conditions (M2), CO<sub>2</sub> net emissions were significantly lower when compressed with 200 kPa compared to 100 kPa at days 5-7

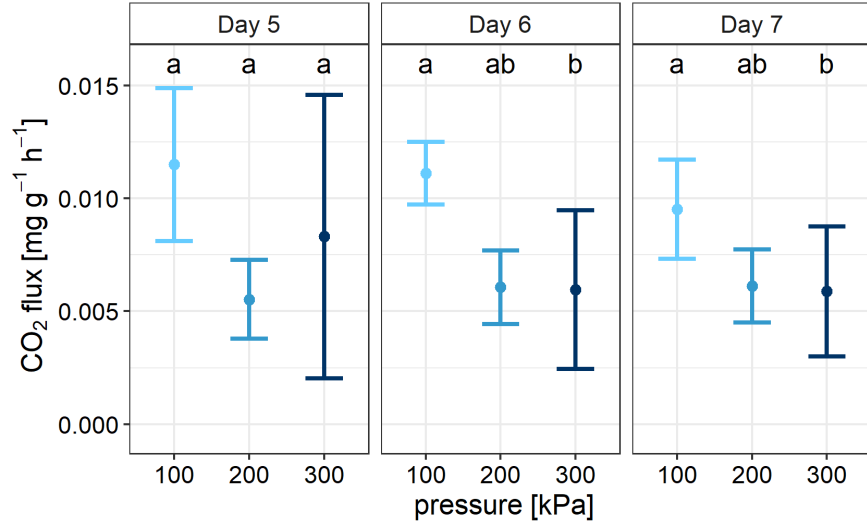


Fig. 10: Differences in mean CO<sub>2</sub> fluxes and standard deviations (n=3) at moist soil conditions (M1) per pressure level (100, 200, 300 kPa) after compaction (Days 5-7). Plot treatment A and C show similar pattern, thus only C is represented in this figure. Letters indicate statistical significances of pairwise comparisons between pressures per day ( $p < 0.05$ ). Significant differences between CO<sub>2</sub> fluxes compacted with 100 and 300 kPa were found on day 6 and 7.

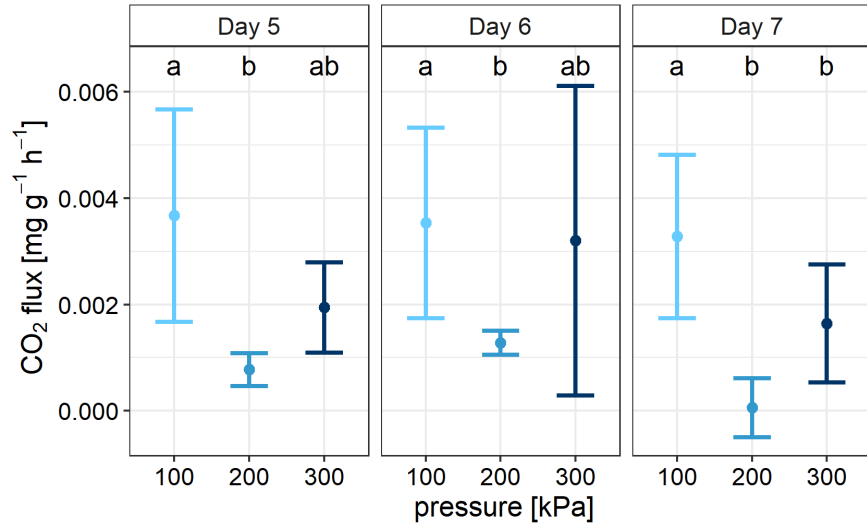


Fig. 11: Differences in mean CO<sub>2</sub> fluxes and standard deviations (n=3) at higher moisture conditions (M2) per pressure level (100, 200, 300 kPa) after compaction (Days 5-7). Plot treatment A and C show similar pattern, therefore only C is represented in this figure. Letters indicate statistical significances of pairwise comparisons between pressures per day ( $p < 0.05$ ). Significant differences between CO<sub>2</sub> fluxes compacted with 100 and 200 kPa were found on all days and 100 and 300 kPa on day 7.

(Fig. 11). Significant differences between 100 and 300 kPa were only found on the seventh day and tendencies at the fifth day. At the seventh day, a trend was observable that CO<sub>2</sub> fluxes were higher when the soil was compacted with 300 kPa compared to 200 kPa. This trend was only observed for M2.

#### **3.2.4 Influence of soil compaction on N<sub>2</sub>O fluxes**

Compaction influenced N<sub>2</sub>O emissions, as fluxes were only detectable on days 5-7. Significant differences for days after compaction were found ( $p = 0.0184$ ). Pairwise comparisons show that N<sub>2</sub>O fluxes on day 5 were significantly higher than on day 6 and 7, respectively ( $p = 0.0195$ ,  $p = 0.028$ ), but no treatment effect was found.

### **3.3 GHG dynamics during compaction**

A typical dynamic of CO<sub>2</sub> concentration before, during and after compaction is shown in Fig. 12, while dynamics of a control sample without compaction is shown in Fig. S1. The grey bars indicate start as well as end of the compaction and show the peak emission of CO<sub>2</sub> when the soil sample was compacted. Comparing the slopes of CO<sub>2</sub> fluxes right before and after compaction, a significant reduction in CO<sub>2</sub> emissions was observed ( $p < 0.0001$ , see Fig. 13). Analogous to the incubator and field measurements, significant differences between plot treatments were found. The control plots A (turquoise) had higher CO<sub>2</sub> emissions compared to C (orange,  $p = 0.0014$ ). The moisture level also influenced CO<sub>2</sub> fluxes ( $p = 0.0001$ ) while different pressures and interactions between factors were not significant.

### **3.4 Influence of compaction on physical properties**

In general, control samples A had approx. 10 % higher porosity compared to plot treatment C ( $p = 0.0016$ ). Figure 14 shows the initial porosity (1 kPa) compared to the porosity after compaction per pressure level. Compaction reduced porosity significantly and was dependent on pressure intensity ( $p < 0.0001$ ). Reduction in porosity was higher when compressed with 300 kPa compared to 100 kPa ( $p < 0.0001$ ). Higher compression led to a higher WFPS ( $p < 0.0001$ ) and depended on plot treatment ( $p = 0.0118$ , Fig. 15). These interactions were not significant in pairwise comparisons. Although control sample A had a higher porosity than C, a significant relationship between plot treatment and WFPS was not observed.

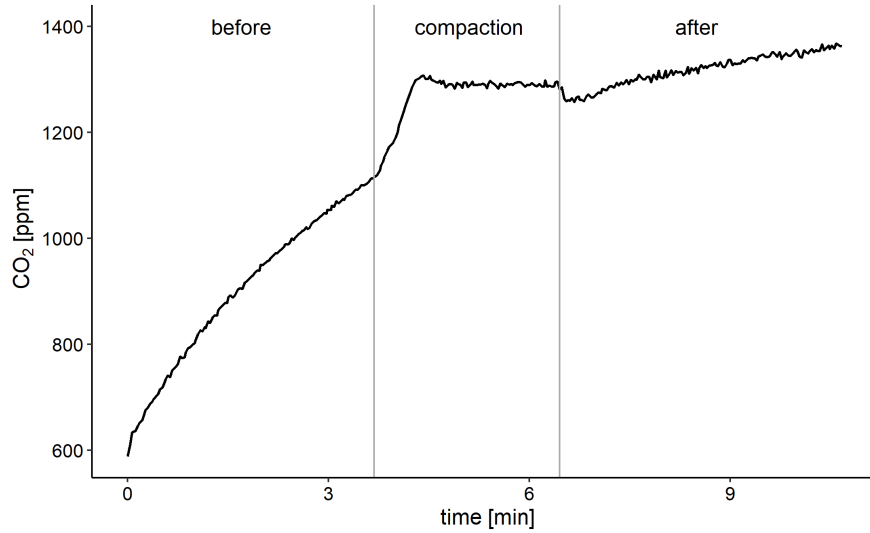


Fig. 12: Example of a typical dynamic in CO<sub>2</sub> concentration [ppm] before, during and after compaction measured in the head-space connected to compression machine. Grey bars indicate the start and end point of the compaction.

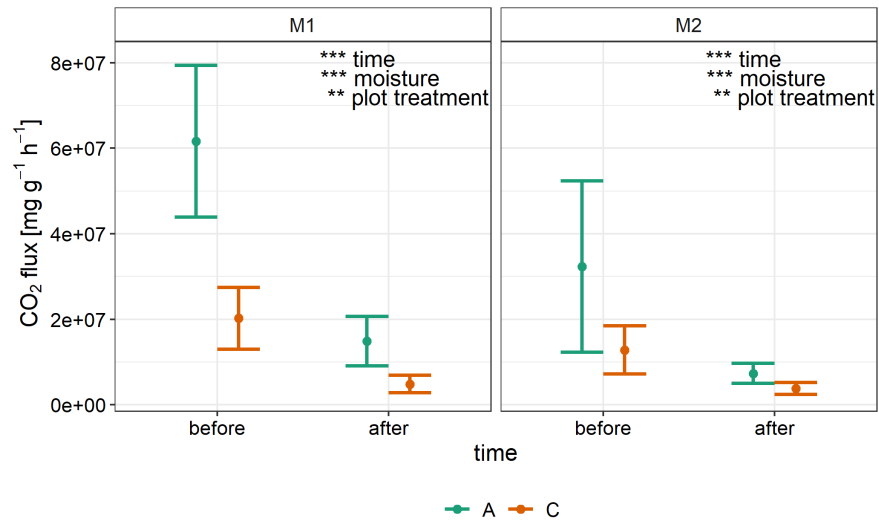


Fig. 13: Differences in mean CO<sub>2</sub> fluxes and standard deviations (n=3) directly before and after compaction with 200 kPa per moisture level (M1, M2) and plot treatment (A, C). Significant reduction in CO<sub>2</sub> emissions after compaction ( $p < 0.0001$ ). Control A had significant higher CO<sub>2</sub> fluxes than C ( $p = 0.0014$ ) and differences between moisture content ( $p = 0.0001$ ). Significant p-values of ANOVA using a linear mixed effect (lme) model: \*\*\*  $< 0.001$ , \*\*  $< 0.01$ , \*  $< 0.05$ .

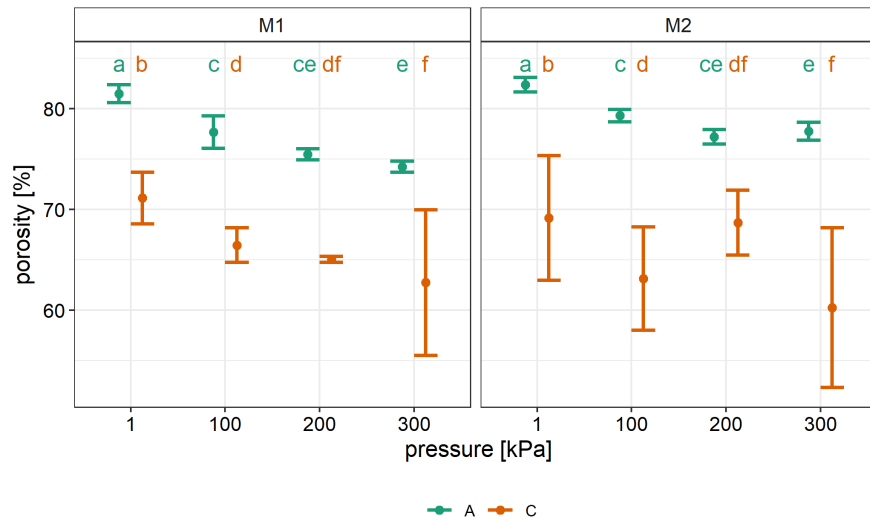


Fig. 14: Differences in mean initial porosity at 1 kPa (n=9) and mean porosity after compaction (n=3) and standard deviations per moisture level (M1, M2) and pressure level (100, 200, 300 kPa). Letters indicate statistical significances of pairwise comparison between plot treatment (A, C) and pressures ( $p < 0.05$ ). Control A (turquoise) had significant higher porosity than C (orange) ( $p = 0.0016$ ) and compaction led to significantly lower porosity ( $p < 0.0001$ ).

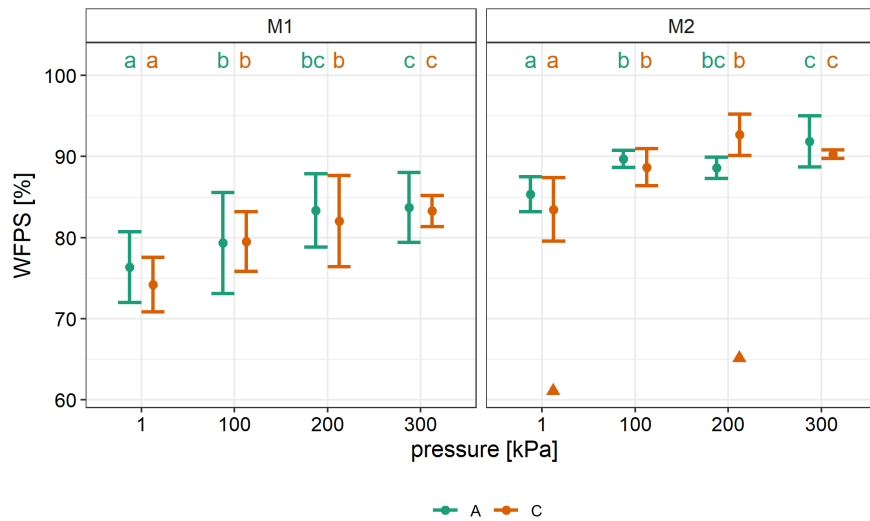


Fig. 15: Differences in mean initial WFPS (water filled pore space) at 1 kPa (n=9) and mean WFPS after compaction (n=3) and standard deviations per moisture level (M1, M2) and pressure level (100, 200, 300 kPa). The triangle marks a potential outlier. Letters indicate statistical significances of pairwise comparison between plot treatment (A, C) and pressures ( $p < 0.05$ ). Higher mechanical loading led to higher WFPS ( $p < 0.0001$ ). No difference between plot treatment was found.

### 3.5 Mechanical properties

Figure 16 shows a typical development of stress during the compaction over time. The compaction stress increased until the target pressure (here 200 kPa) was reached. Then the piston stayed in place for the holding time of 120 seconds while no additional stress was applied. Thus, the soil relaxes and the measured stress decreased. The corresponding compression curve to Fig. 16 is shown in the upper part of Fig. 17. The continuous black line is the loading path with the grey dots indicating the measuring points. The red line indicates the virgin compression line and its slope determined as  $C_c$ . The blue line indicates the unloading path, the swelling line, which is the elastic and reversible behaviour of peat soils after stress release, whereas the slope is termed  $C_s$ . Comparing the compression curves presented in Fig. 17, both indices ( $C_c$  and  $C_s$ ) were larger for plot treatment A than for C ( $p < 0.0001$ ). The (re-)compression behaviour of natural peat soils (A) was approximately twice as high as peat with sand addition (C, see table 4). The average value for  $C_s$  of 0.21 (0.10) implies that unloading to 1 kPa leads to an average increase in void ratio of 0.51 (0.24). Intensity of applied stress and moisture level did not have a significant influence on the (re-)compression behaviour of peat soils.

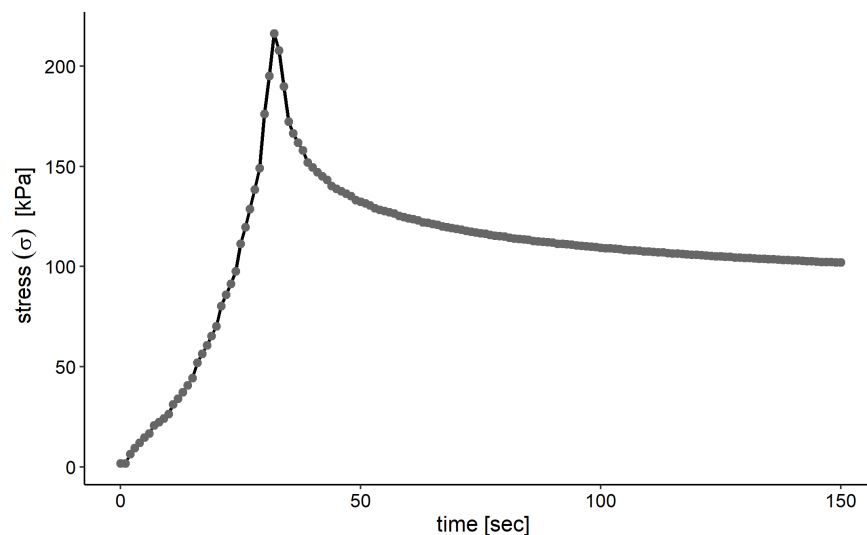


Fig. 16: Example of the measured applied stress during compaction over time. After the target pressure (here 200 kPa) was reached the piston stayed in that position for 120 seconds without applying further vertical stress on the soil core.

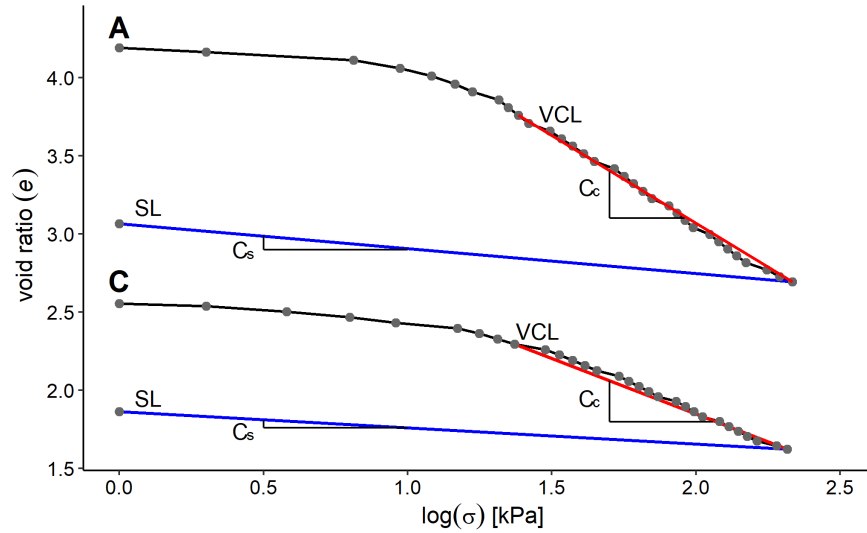


Fig. 17: Example of a measured compression curve as a function of void ratio ( $e$ ) and the logarithm of applied stress ( $\sigma$ ) for plot treatment A (upper curve) and C (lower curve). Grey points indicate the measured values while the red and blue line, respectively express the virgin compression line (VCL) and swelling line (SL). The slopes of the virgin compression line and swelling line are termed  $C_c$  and  $C_s$ . Both indices  $C_c$  and  $C_s$  were larger for A than C ( $p < 0.0001$ ), indicating lower compressibility and rebound for peat soils with sand addition.

Table 4: Compression and recompression index  $C_c$  and  $C_s$  per plot treatment A and C. Significant differences between plot treatment indicated with significant level. P-values of Kruskal Wallis test: \*\*\*  $< 0.001$ , \*\*  $< 0.01$ , \*  $< 0.05$ .

	Treatment A	Treatment C	Significance level
$C_c$	0.54 ( $\pm 0.12$ )	0.26 ( $\pm 0.08$ )	***
$C_s$	0.21 ( $\pm 0.06$ )	0.10 ( $\pm 0.03$ )	***

Positive correlation between  $C_c$  and initial void ratio  $e_0$  was found, as shown by the linear regression equation 9. The correlation between  $C_c$  and  $e_0$  was slightly stronger than that between  $C_s$  and  $e_0$  (equation 10). No further linear relationships between mechanical properties and soil properties were found.

$$C_c = -0.068(\pm 0.048) + 0.135(\pm 0.132) * e_0 \quad R^2 = 0.75, p < 0.0001 \quad (9)$$

$$C_s = -0.024(\pm 0.026) + 0.053(\pm 0.007) * e_0 \quad R^2 = 0.62, p < 0.0001 \quad (10)$$

## 4 Discussion

### 4.1 Influence of sand addition on CO<sub>2</sub> emissions

Laboratory and field measurements of this study show that sand addition leads to significantly lower CO<sub>2</sub> emissions. These findings align with the measurements conducted 2017-2019 at the same field site (Ö. Berglund 2020). Comparing absolute CO<sub>2</sub> fluxes from samples of control and peat soil with sand addition a significant reduction in CO<sub>2</sub> emissions in field and laboratory experiments were observable. In contrast, there was no difference when specific CO<sub>2</sub> fluxes of both treatments were compared (see figures S2, S3). The specific CO<sub>2</sub> flux is normalized to the  $C_{org}$  content and the non-significant difference in specific CO<sub>2</sub> flux from peat with and without sand addition indicates that the degradation rate of peat soils was not reduced by incorporation of sand. This implies that organic matter of the samples with sand addition was not stable, which aligns with studies conducted on a bog peat with sand addition (Säurich et al. 2019). The decrease in  $C_{org}$  content due to sand addition might be the reason for the reduction of the absolute CO<sub>2</sub> emissions found in the field and laboratory experiment as higher mineral content in peat soil leads to higher macropore contents (Walczak et al. 2002). This change in pore size distribution affects the water retention characteristics (Walczak et al. 2002; Frey et al. 2009), but might also influence gas fluxes. Interestingly, comparing both plot treatments, a significant difference in porosity ( $p = 0.0016$ ) was found, but not for WFPS. Therefore, porosity might be a better predictor than WFPS for altered gas fluxes due to sand addition. Although, changes in pore size distribution should be considered in future studies. According to Höper (2015) lower CO<sub>2</sub> emissions of sand addition can only be expected on cultivated grasslands. Because of ploughing in agricultural management, cultivated fields with sand addition have similar emission as agricultural peatlands without sand incorporation. Therefore, more studies with various peat types and different amounts of sand addition under different agricultural managements are necessary to identify, whether the reduction of  $C_{org}$  in the topsoil, leading to changes in physical properties, might promote a stabilization of the soil organic matter. This stabilization is crucial for an efficient management practice to protect peat soils from degradation.

### 4.2 Influence of soil compaction on CO<sub>2</sub> emissions

This study shows that soil compaction reduces the CO<sub>2</sub> emissions. After the outgassing effect during compaction described by Mordhorst et al. (2014), the CO<sub>2</sub> reduction was observed directly after compaction as well as during the measuring period of three days. These findings align with studies conducted

on cultivated, mineral soils (Teepe et al. 2004; Ruser et al. 2006; Gregory et al. 2007; Frey et al. 2009; Weisskopf et al. 2010; Mordhorst et al. 2014), but are contradictory to Busman et al. (2021), who indicated higher CO<sub>2</sub> fluxes at higher bulk densities over a 12 week measuring period for peat soils. Next to the longer measuring period, the chosen bulk densities were lower (0.14 - 0.22 g cm<sup>-3</sup>) than in this study (treatment A: initial 0.3 ± 0.02 g cm<sup>-3</sup>, final 0.34 ± 0.03 g cm<sup>-3</sup>). Lower initial bulk densities are due to lower degradation degree (H5-H6 to H9-H10) and different peat types (forest swamp peat to fen peat). Compaction leads to an increase in bulk density and a decrease in porosity (Ball et al. 2008). Although, bulk density and porosity are not a good indicator for assessing the influence of compaction stress on microbial activity due to changes in soil aeration and water flow (Young and Ritz 2000). A small variation in total porosity (bulk density) due to compaction can have a high variability in pore size distribution, changing the relative proportion of micropores and macropores (Verry et al. 2011). Compaction reduces the amount and continuity of macropores, which controls water and air flow (McNabb et al. 2001; Frey et al. 2009), leading to an enhanced capillary rise and water retention capacity (Melling et al. 2014). This results in higher WFPS, which affects CO<sub>2</sub> fluxes. Topsoil peat respiration is maximal at medium WFPS. When this optimum is exceeded, the microbial respiration and decomposition rate of organic matter decreases leading to lower net CO<sub>2</sub> fluxes from soils (Doran et al. 1990; Husen et al. 2014; Melling et al. 2014). Optimal WFPS for soil respiration is dependent on soil texture and highest CO<sub>2</sub> emissions occur in different mineral soils at WFPS between 40 - 70 % (Linn and Doran 1984; Doran et al. 1990). For peat soils, maximal CO<sub>2</sub> emissions were reported at 50 % (Husen et al. 2014) and 60 - 70 % WFPS (Lent et al. 2019). In this study, it can be assumed that the initial WFPS (> 70 %) was already higher than the optimal WFPS value for soil respiration. Therefore, the reduction in CO<sub>2</sub> emissions due to compaction can be explained by the increase in WFPS. This can also be seen by comparing both moisture levels, where slightly higher water contents resulted in lower CO<sub>2</sub> emissions. However, when WFPS is below the reported optimum (eg. 60 %), an increase in WFPS enhances microbial population and respiration (Linn and Doran 1984; Husen et al. 2014). Under realistic field conditions, it is very likely that WFPS lies below that limit, because of limited trafficability at wet conditions. Therefore, peat soil compaction could lead to higher CO<sub>2</sub> emissions when initial WFPS are below 60 %. More studies with different initial water contents are necessary to understand the impact of soil compaction on GHG fluxes. It is also recommended that soil cores are drained on a sand bed to defined water retentions. This method can effectively create different moisture levels and is less disturbing than drying the samples at 30 °C. In this study, the air-drying method at 30 °C was chosen because of time limitations.

### **4.3 Influence of different mechanical loading on CO<sub>2</sub> fluxes**

Differences in mechanical loading on CO<sub>2</sub> fluxes were found in the incubator measurements, three days following compaction. Although the results show an unclear pattern, especially at higher moisture conditions (M2). There, differences between 100 and 200 kPa were found every day and a trend for significant differences between all pressures at day 7 was observed. It was unexpected that CO<sub>2</sub> fluxes seem to be higher when compacted with 300 kPa compared to 200 kPa. However, this might be due to an outlier at compaction pressure 200 kPa. It is difficult to remove outliers due to the small sample size (three per treatment group). Therefore, a bigger sample size would be necessary to deal with outliers and to have higher statistical power. At lower moisture conditions (M1), there was a significant difference between 100 and 300 kPa, indicating a higher reduction of CO<sub>2</sub> emissions at higher mechanical loading. This aligns with Frey et al. (2009), where high loading intensity lead to a higher disturbance and lower CO<sub>2</sub> emissions, while at low and moderate loading an adequate air-filled porosity maintains ecological functions. This could also explain the non-significant effect of soil compaction with 100 kPa on CO<sub>2</sub> fluxes at lower moisture conditions (M1, see Fig. S4). Furthermore, there were tendencies that higher intensity of mechanical loading affected porosity ( $p < 0.1$  for 100-300 kPa and 200-300 kPa). Larger differences in pressure might have led to a more differentiated result.

However, Clay and Worrall (2013) show that the presence of compaction is more important than the intensity. Peat soil CO<sub>2</sub> emissions are reduced by up to 75 % by sheep trampling. This effect is reversed when sheep trampling is stopped (Clay and Worrall 2013). Although effects of compaction by animals and vehicles are difficult to compare, because of the different disturbance regimes, recovery properties of peat soils after disturbance might play an important role for further studies. At the field site in Broddbo an ongoing compaction field trial is conducted. One year after the mechanical compaction the initial difference in penetration resistance between control and compaction plot was no longer measurable (Ö. Berglund 2021). It is currently studied, if this single compaction event last year had a long-term effect on GHG emissions. Furthermore, Busman et al. (2021) describe that the effect of bulk density on CO<sub>2</sub> fluxes changed over the twelve week measuring period. Samples with higher bulk density had higher CO<sub>2</sub> fluxes in week 0-8 and lower during week 9-12 compared to less compacted samples. Therefore, long-term incubation and field studies are necessary to understand changes of GHG fluxes after compaction. Thereby, additional soil microbiological analysis techniques could complement GHG measurements to assess short- and long-term responses of microbial communities to soil compaction. This could help understanding the effects of higher disturbance by heavier machinery on soil microbial communities and

ecosystem functioning, which is important to explain altered GHG fluxes. Further studies with different cultivated peatlands are needed due to the high heterogeneity of peat soils. Furthermore, it would be interesting to analyze recompaction of peat soils to simulate multiple passes of a tractor and its effect on CO<sub>2</sub> fluxes.

#### **4.4 Influence of soil compaction on N<sub>2</sub>O fluxes**

Nitrous oxide fluxes above detection limit were only found in incubator measurements after compaction. These were highest on day 5 suggesting that compaction leads to hot moments in N<sub>2</sub>O emissions. Higher WFPS due to compaction enhanced denitrification and hence N<sub>2</sub>O emissions. Nevertheless, these findings have to be treated cautiously, as only 36 % of the samples had measurable N<sub>2</sub>O fluxes after compaction. No further treatment effects could be observed because of the small sample size with detectable N<sub>2</sub>O fluxes. This reflects the high heterogeneity of peats and temporal variability of N<sub>2</sub>O emissions.

#### **4.5 Improvement of GHG measurements during compaction**

An important part of this study was to develop a method to observe GHG dynamics during compaction, as this has been rarely studied. The soda lime experiment showed that the chosen set-up was air-tight and leakage could be neglected. The rubber was a suitable solution because of its elastic properties. It fitted around the piston perfectly and mitigated leakage (see Fig 4). A plastic ring covered the sharp edges of the cylinder bottom to prevent ripping of the condom. However, the system is still very sensitive to ripping and it has to be tested when higher pressures and loading speeds are applied. When higher pressures (eg. 500 kPa) and loading speeds are used, it should be considered not to use too wet soils, as excess water accumulates in the system and increases the risk of the rubber breaking. Furthermore, excess water which leaves the soil core is lost and might affect the following GHG measurements and the precision of the parameter calculations.

Flushing of the system after compaction measurement with ambient air took a very long time and usually CO<sub>2</sub> concentrations did not drop below 500 ppm. Therefore, the initial CO<sub>2</sub> concentration in the consecutive measurement was already high. Flushing the system with soda lime instead of ambient air could resolve this problem and improve workflow.

In pre-tests, a loading rate of 1 mm/sec and pressures up to 500 kPa were tested. However, higher loading rate and pressures regularly led to an over-compaction over 10 %, meaning that the target pressure was exceeded. This could be because of the strong stiffness of organic soils at large compaction pressures

(Den Haan 1997). In order to minimize over-compaction, the loading rate was reduced to 0.5 mm/sec and applied stresses between 100-300 kPa.

#### **4.6 Mechanical behaviour of peat soils**

In general, peat soils have higher (re-)compression properties than mineral soils. One reason is the high initial void ratio of peat soils leading to a large deformation when mechanical loading is applied (ElMouchi et al. 2021). Positive correlations between initial void ratio and mechanical properties  $C_c$  and  $C_s$  were found, indicating higher deformation and rebound behaviour to external loading at higher void ratio. Secondly, compression and recompression behaviour are dependent on soil organic carbon content (Yamaguchi et al. 1985; Zhang et al. 2005; Kuan et al. 2007). Although no linear relationship between organic matter content and  $C_c$  and  $C_s$  was found, a difference in plot treatment was observed. Sand addition led to an improvement of soil resistance (lower  $C_c$ ), while the rebound after compression was reduced (lower  $C_s$ ).

According to literature  $C_c$  ranges between 0.5 and 18 for organic soils because of the high initial void ratio (Lefebvre et al. 1984; Yamaguchi et al. 1985; Ajlouni 2000; Abdel Kadar 2010; Vennik et al. 2019). In this experiment, the mean  $C_c$  was 0.57 (A) and 0.25 (C) ranking in the lower range of the suggested scale. Estimation of  $C_c$  could be improved, if void ratio and corresponding mean vertical stress were fitted with the Gompertz equation. The fitted model could then be used to calculate the corresponding compressive property  $C_c$  (O'Sullivan 1996; Gregory et al. 2006; Vennik et al. 2019). Furthermore,  $C_c$  is dependent on applied compaction stress, initially increasing with increased stress and decreasing when twice the precompression stress is exceeded (Yamaguchi et al. 1985; Mesri et al. 1997; ElMouchi et al. 2021). In this study,  $C_c$  was not influenced by different stress intensities. This could be due to relative small difference between the applied pressures compared to common compaction studies (Keller et al. 2011; Madaschi and Gajo 2015; Yang et al. 2016; Vennik et al. 2019). Estimated  $C_s$  seemed very low and was one magnitude lower than Vennik et al. (2019) reported for another peat soil. One reason could be the high variability between different peat types, or due to the higher intensity of applied stress, which was 2.8-8.5 times higher than in this study. Compression and especially recompression behaviour of organic soils due to vehicular traffic is little studied. Therefore, more research is necessary to investigate the mechanical compressive behaviour of different peat types. Furthermore, it is important to consider rate-dependent and viscous behaviour of peat, when mechanical behaviour is examined (Yang et al. 2016). This study did not account for either of these and this should be subject of further studies.

## 5 Conclusions

This study showed that sand addition could be a good management practice to reduce CO<sub>2</sub> emission of peat soils, while improving soil physical properties. Contrary to the findings of Busman et al. (2021), soil compaction led to a reduction in CO<sub>2</sub> emission after a short-term burst effect. This might be due to very high initial WFPS and an opposite effect on CO<sub>2</sub> fluxes could be plausible at lower water contents, simulating more realistic field conditions for vehicular traffic. Therefore, more studies with different water contents are crucial to understand the influence of compaction on GHG fluxes. Higher intensity of mechanical loading does not necessarily result in a higher effect on CO<sub>2</sub> emissions. The trend of CO<sub>2</sub> emissions after applying different pressures (100, 200 and 300 kPa) was unclear. This could be due to limited statistical power, but can also imply that the presence of compaction might be more important than the intensity. Furthermore, compaction might lead to hot moments in N<sub>2</sub>O emissions. The developed set-up of in-situ GHG measurements during compaction worked and the dynamics of CO<sub>2</sub> emission could be observed. After small adjustments, this method could be used for further research, studying changes in GHG emissions due to compression. Mechanical properties of peat soils were influenced by sand incorporation. Sand addition reduced soil compressibility ( $C_c$ ) as well as rebound after stress release ( $C_s$ ). Linear relationships between initial void ratio and compressive indices  $C_c$  and  $C_s$  were found, but not for other soil properties. Accurate prediction of the mechanical behaviour of peat soils during vehicular traffic is highly relevant and little understood. There is a great need for further research to accurately estimate mechanical behaviour to vehicular traffic. Further studies should include experiments with multiple loading steps and loading rates to account for rate-dependant and viscous behaviour of peat soils.

## Acknowledgments

The project was part of 4.1.18-18808/2020 and was financed by the Swedish Board of Agriculture. Furthermore, I like to thank everybody involved in this project and helping me conducting this Master thesis. Special thanks to my main supervisor Örjan Berglund and Sabine Jordan for introducing me to peat soils. Daniel Ileskog thank you very much for developing the method to measure GHG within "Ceasar" with me and for all the good jokes finding the right rubber for the measurements. Thank you, Thomas Keller for the insights on soil mechanics and good discussions about my results. Kerstin Berglund for your good feedback in your peer review as well as many thanks to intern Leon Schröder for your support in conducting the field measurements. I would also like to acknowledge the co-supervision of Mr Thilo Streck from my home university in Hohenheim.

## Supplementary Material

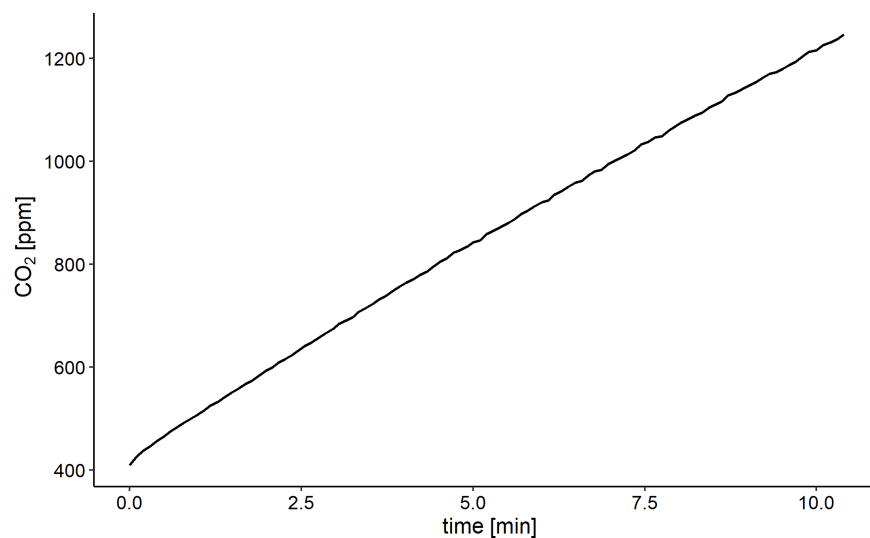


Fig. S1: Dynamics of CO<sub>2</sub> concentration [ppm] without compaction measured in head-space connected to the compression machine,  $R^2 = 0.99$ ,  $p < 0.0001$ .

Table S1: Significant treatment effect of soil compaction indicated by p-values of ANOVA with linear mixed effect (lme) model between measured days per plot treatment (A, C), moisture level (M1, M2) and pressure level (100, 200 and 300 kPa). Significant p-values: \*\*\* &lt; 0.001, \*\* &lt; 0.01, \* &lt; 0.05 and n.s &gt; 0.05.

Days	Treatment A						Treatment C					
	Moisture level M1			Moisture level M2			Moisture level M1			Moisture level M2		
	100 kPa	200 kPa	300 kPa	100 kPa	200 kPa	300 kPa	100 kPa	200 kPa	300 kPa	100 kPa	200 kPa	300 kPa
1/2	n.s	n.s	n.s									
1/3	n.s	n.s	n.s	0.015	n.s	0.005	n.s	n.s	n.s	0.095	n.s	0.041
1/5	n.s	0.015	0.011	<.0001	<.0001	<.0001	n.s	0.012	0.021	<.0001	<.0001	<.0001
1/6	n.s	n.s	0.018	<.0001	<.0001	<.0001	n.s	0.049	0.001	0.003	<.0001	<.0001
1/7	n.s	n.s	0.005	0.006	<.0001	<.0001	n.s	0.079	0.002	0.001	<.0001	<.0001
2/3	n.s	n.s	n.s	0.03	n.s	0.006	n.s	n.s	n.s	0.009	n.s	0.001
2/5	n.s	0.004	0.001	<.0001	<.0001	<.0001	n.s	0.006	0.003	<.0001	<.0001	<.0001
2/6	n.s	n.s	0.002	<.0001	<.0001	<.0001	n.s	0.036	<.0001	0.001	<.0001	<.0001
2/7	n.s	n.s	<.0001	0.045	<.0001	<.0001	n.s	0.063	<.0001	<.0001	<.0001	<.0001
3/5	n.s	<.0001	<.0001	0.041	<.0001	<.0001	n.s	<.0001	<.0001	0.055	<.0001	<.0001
3/6	n.s	0.04	<.0001	0.04	<.0001	<.0001	n.s	0.001	<.0001	n.s	<.0001	0.003
3/7	n.s	0.028	<.0001	n.s	<.0001	<.0001	n.s	0.003	<.0001	n.s	<.0001	<.0001
5/6	n.s	n.s	n.s	n.s	n.s	n.s	n.s	n.s	n.s	n.s	n.s	0.042
5/7	n.s	n.s	n.s	n.s	n.s	n.s	n.s	n.s	n.s	n.s	0.027	n.s
6/7	n.s	n.s	n.s	0.068	n.s	n.s	n.s	n.s	n.s	n.s	<.0001	<.0001

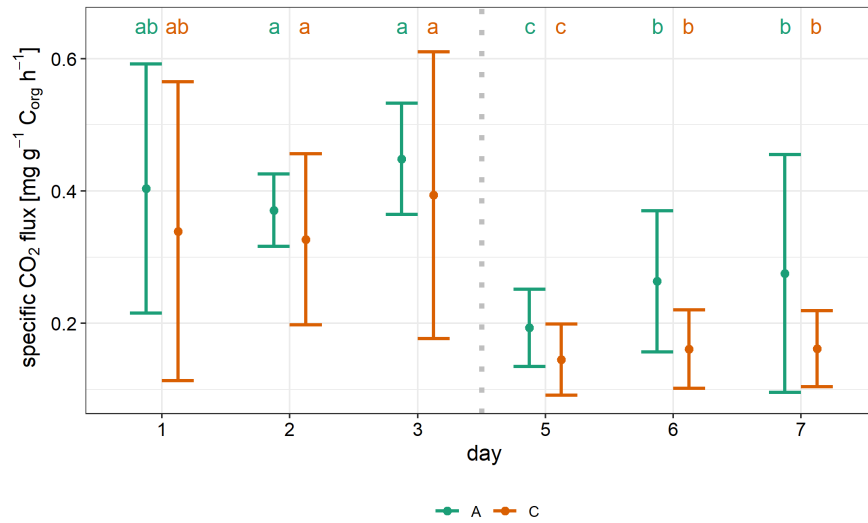


Fig. S2: Mean specific CO<sub>2</sub> flux (n=3) and standard deviations per plot treatment at lower moisture conditions (M1). Compaction with 200 kPa at day 4 indicated with dotted line. Letters indicate statistical significances of pairwise comparisons between treatments and days ( $p < 0.05$ ). Specific CO<sub>2</sub> flux was calculated by normalizing gas flux with corresponding  $C_{org}$  content of dry soil weight. Thereby, no significant difference between specific CO<sub>2</sub> flux of control (A, orange) and samples with sand addition (C, turquoise) was found.

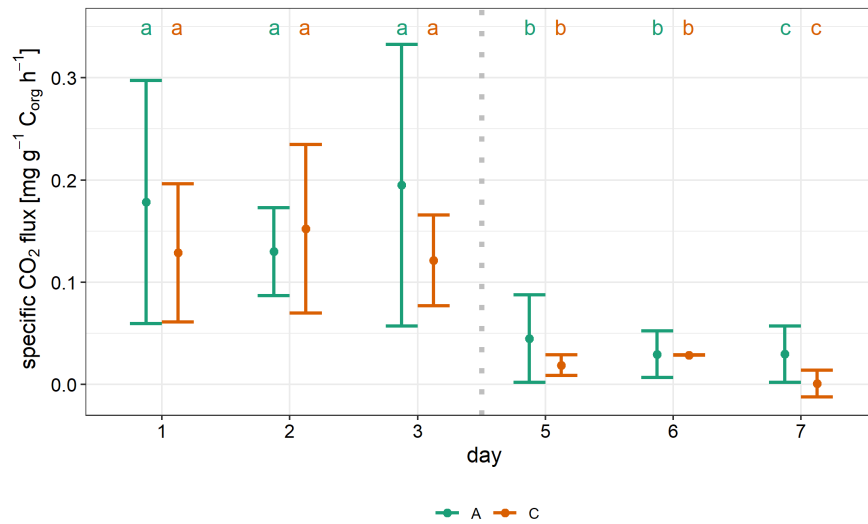


Fig. S3: Mean specific CO<sub>2</sub> flux (n=3) and standard deviations per plot treatment at lower moisture conditions (M2). Compaction with 200 kPa at day 4 indicated with dotted line. Letters indicate statistical significances of pairwise comparisons between treatments and days ( $p < 0.05$ ). Specific CO<sub>2</sub> flux was calculated by normalizing gas flux with corresponding  $C_{org}$  content of dry soil weight. Thereby, no significant difference between specific CO<sub>2</sub> flux of control (A, orange) and samples with sand addition (C, turquoise) was found.

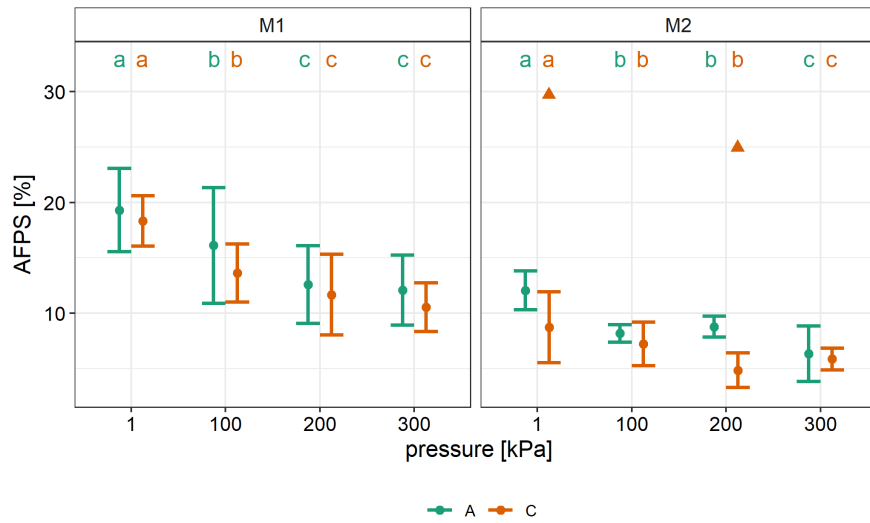


Fig. S4: Differences in mean initial air-filled pore space (AFPS = porosity-VWC) at 1 kPa (n=9) and mean AFPS after compaction (n=3) as well as standard deviations per moisture level (M1, M2) and pressure level (100, 200, 300 kPa). The triangle marks a potential outlier. Letters indicate statistical significances of pairwise comparison between plot treatment (A, C) and pressures ( $p < 0.05$ ). Linear mixed-effect model of ANOVA included factors plot treatment and interaction of pressure and moisture level. Higher mechanical loading led to higher AFPS ( $p < 0.0001$ ). No difference between plot treatment was found.

## References

- Abdel Kadar, HI (2010). "Compressibility Characteristics of Organic Soils in Egypt". *MSc Thesis Department of Public Works, Cairo University*.
- Ajlouni, M. A. (2000). "Geotechnical Properties of Peat and Related Engineering Problems". *PhD Thesis Department of Civil Engineering, University of Illinois*.
- Arvidsson, Johan and Thomas Keller (2007). "Soil stress as affected by wheel load and tyre inflation pressure". *Soil and Tillage Research* 96.1-2, pp. 284–291. doi: 10.1016/j.still.2007.06.012.
- Asselen, S. van, E. Stouthamer, and Th.W.J. van Asch (2009). "Effects of peat compaction on delta evolution: A review on processes, responses, measuring and modeling". *Earth-Science Reviews* 92.1-2, pp. 35–51. doi: 10.1016/j.earscirev.2008.11.001.
- Ball, B, I Crichton, and G Horgan (2008). "Dynamics of upward and downward N<sub>2</sub>O and CO<sub>2</sub> fluxes in ploughed or no-tilled soils in relation to water-filled pore space, compaction and crop presence". *Soil and Tillage Research* 101.1-2, pp. 20–30. doi: 10.1016/j.still.2008.05.012.
- Beare, M.H., E.G. Gregorich, and P. St-Georges (2009). "Compaction effects on CO<sub>2</sub> and N<sub>2</sub>O production during drying and rewetting of soil". *Soil Biology and Biochemistry* 41.3, pp. 611–621. doi: 10.1016/j.soilbio.2008.12.024.
- Berglund, Kerstin (1996). *Cultivated organic soils in Sweden: properties and amelioration*. Swedish University of Agricultural Sciences, Department of Soil Sciences, Uppsala 28. OCLC: 35167054. Uppsala.
- Berglund, Örjan (2011). "Greenhouse Gas Emissions from Cultivated Peat Soils in Sweden". *Doctoral thesis, Sveriges lantbruksuniversitetet, Acta Universitatis Agriculturae Sueciae*, ISBN 978-91-576-7571-2, pp. 1–72.
- Berglund, Örjan (2020). "Åtgärder för att minska växthusgasavgången och öka skörden från odlade organogena jordar". Sveriges landbruksuniversitet, Uppsala, Slutrapport 4.1.18-9995/16, pp. 1–25.
- Berglund, Örjan (2021). *Measurement of penetration resistance on compaction trial in Broddbo 2020-2021*. Personal communication at 15.07.2021.
- Berglund, Örjan and Kerstin Berglund (2011). "Influence of water table level and soil properties on emissions of greenhouse gases from cultivated peat soil". *Soil Biology and Biochemistry* 43.5, pp. 923–931. doi: 10.1016/j.soilbio.2011.01.002.
- Bridgman, Scott D., Hinsby Cadillo-Quiroz, Jason K. Keller, and Qianlai Zhuang (2013). "Methane emissions from wetlands: biogeochemical, microbial, and modeling perspectives from local to global scales". *Global Change Biology* 19.5, pp. 1325–1346. doi: 10.1111/gcb.12131.

- Busman, Nur Azima, Nagamitsu Maie, Che Fauziah Ishak, Muhammad Firdaus Sulaiman, and Lulie Melling (2021). "Effect of compaction on soil CO<sub>2</sub> and CH<sub>4</sub> fluxes from tropical peatland in Sarawak, Malaysia". *Environment, Development and Sustainability* 23.8, pp. 11646–11659. doi: 10.1007/s10668-020-01132-y.
- Canakci, Hanifi, Fatih Celik, and Tuncer B. Edil (2019). "Effect of sand column on compressibility and shear strength properties of peat". *European Journal of Environmental and Civil Engineering* 23.9, pp. 1094–1105. doi: 10.1080/19648189.2017.1344142.
- Clay, Gareth D. and Fred Worrall (2013). "The response of CO<sub>2</sub> fluxes from a peat soil to variation in simulated sheep trampling". *Geoderma* 197-198, pp. 59–66. doi: 10.1016/j.geoderma.2012.12.008.
- DeLuca, T. H., D. R. Keeney, and G. W. McCarty (1992). "Effect of freeze-thaw events on mineralization of soil nitrogen". *Biology and Fertility of Soils* 14.2, pp. 116–120. doi: 10.1007/BF00336260.
- Den Haan, E. J. (1997). "An overview of mechanical behaviour of peats and organic soils and some appropriate construction techniques". *Conference on Recent Advances in Soft Soil Engineering, Sarawak*, pp. 17–45.
- Doran, J. W., L. N. Mielke, and J. F. Power (1990). "Microbial activity as regulated by soil water-filled pore space". Vol. Volume III. Kyoto, Japan, pp. 94–99.
- EIMouchi, Ahmed, Sumi Siddiqua, Dharma Wijewickreme, and Herbert Polinder (2021). "A Review to Develop new Correlations for Geotechnical Properties of Organic Soils". *Geotechnical and Geological Engineering* 39.5, pp. 3315–3336. doi: 10.1007/s10706-021-01723-0.
- FAO (2014). *World reference base for soil resources 2014: international soil classification system for naming soils and creating legends for soil maps*. OCLC: 1004475995. Rome: FAO.
- Firestone, M.K. and E.A. Davidson (1989). "Microbiological Basis of NO and N<sub>2</sub>O Production and Consumption in Soils. In: Andreae, M.O. and Schimel". *Exchange of Trace Gases between Terrestrial Ecosystems and the Atmosphere, John Willey and Sons, New York*, pp. 7–21.
- Frey, Beat, Johann Kremer, Andreas Rüdte, Stephane Sciacca, Dietmar Matthies, and Peter Lüscher (2009). "Compaction of forest soils with heavy logging machinery affects soil bacterial community structure". *European Journal of Soil Biology* 45.4, pp. 312–320. doi: 10.1016/j.ejsobi.2009.05.006.
- Gregory, A.S., C.W. Watts, W.R. Whalley, H.L. Kuan, B.S. Griffiths, P.D. Hallett, and A.P. Whitmore (2007). "Physical resilience of soil to field compaction and the interactions with plant growth and microbial community structure". *European Journal of Soil Science* 58.6, pp. 1221–1232. doi: 10.1111/j.1365-2389.2007.00956.x.

- Gregory, A.S., W.R. Whalley, C.W. Watts, N.R.A. Bird, P.D. Hallett, and A.P. Whitmore (2006). "Calculation of the compression index and precompression stress from soil compression test data". *Soil and Tillage Research* 89.1, pp. 45–57. doi: 10.1016/j.still.2005.06.012.
- Höper, Heinrich (2015). "Treibhausgasemissionen aus Mooren und Möglichkeiten der Verringerung". TEL-MA. Beiheft 5, pp. 133–158.
- Husen, Edi, Selly Salma, and Fahmuddin Agus (2014). "Peat emission control by groundwater management and soil amendments: evidence from laboratory experiments". *Mitigation and Adaptation Strategies for Global Change* 19.6, pp. 821–829. doi: 10.1007/s11027-013-9526-3.
- Joosten, Hans and Donal Clarke (2002). *Wise use of mires and peatlands: background and principles including a framework for decision-making*. OCLC: ocm51393261. International Peat Society and International Mire Conservation Group.
- Jordan, Sabine (2016). "Greenhouse Gas Emissions from Rewetted Extracted Peatlands in Sweden". *Doctoral thesis, Sveriges lantbruksuniversitetet, Acta Universitatis Agriculturae Sueciae*, ISBN 978-91-576-8707-4, pp. 1–102.
- Keller, Thomas, Johan Arvidsson, Per Schjønning, Mathieu Lamande, Matthias Stettler, and Peter Weiskopf (2012). "In Situ Subsoil Stress-Strain Behavior in Relation to Soil Precompression Stress". *Soil Science* 177.8, pp. 490–497.
- Keller, Thomas, Mathieu Lamandé, Per Schjønning, and Anthony R. Dexter (2011). "Analysis of soil compression curves from uniaxial confined compression tests". *Geoderma* 163.1-2, pp. 13–23. doi: 10.1016/j.geoderma.2011.02.006.
- Kuan, H. L., P. D. Hallett, B. S. Griffiths, A. S. Gregory, C. W. Watts, and A. P. Whitmore (2007). "The biological and physical stability and resilience of a selection of Scottish soils to stresses". *European Journal of Soil Science* 58.3, pp. 811–821. doi: 10.1111/j.1365-2389.2006.00871.x.
- Lefebvre, G, P Langlois, and C Lupien (1984). "Laboratory testing and in situ behaviour of peat as embankment foundation". *Canadian Geotechnical Journal*. Volume 21, pp. 322–337.
- Lennartz, Bernd and Haojie Liu (2019). "Hydraulic Functions of Peat Soils and Ecosystem Service". *Frontiers in Environmental Science* 7, pp. 1–5. doi: 10.3389/fenvs.2019.00092.
- Lent, Jeffrey van, Kristell Hergoualc'h, Louis Verchot, Oene Oenema, and Jan Willem van Groenigen (2019). "Greenhouse gas emissions along a peat swamp forest degradation gradient in the Peruvian Amazon: soil moisture and palm roots effects". *Mitigation and Adaptation Strategies for Global Change* 24.4, pp. 625–643. doi: 10.1007/s11027-018-9796-x.

- Lenth, Russell (2020). *Estimated Marginal Means, aka Least-Squares Means*. url: <https://CRAN.R-project.org/package=emmeans>.
- Linn, D. M. and J. W. Doran (1984). "Effect of Water-Filled Pore Space on Carbon Dioxide and Nitrous Oxide Production in Tilled and Nontilled Soils". *Soil Science Society of America Journal* 48.6, pp. 1267–1272. doi: 10.2136/sssaj1984.03615995004800060013x.
- Madaschi, A. and A. Gajo (2015). "One-dimensional response of peaty soils subjected to a wide range of oedometric conditions". *Géotechnique* 65.4, pp. 274–286. doi: 10.1680/geot.14.P.144.
- Mäkilä, Markku and Tomasz Goslar (2008). "The carbon dynamics of surface peat layers in southern and central boreal mires of Finland and Russian Karelia". *Suo* 59(3):49-69, pp. 49–69.
- Mattsson, Andreas (2018). "Växthusgasutsläpp vid sandinblandning i torvjordar". Sveriges lantbruksuniversitet, Uppsala, pp. 1–15.
- McCoy, E L (1998). "Sand and Organic Amendment Influences on Soil Physical Properties Related to Turf Establishment". *AGRONOMY JOURNAL* 90, pp. 411–419.
- McNabb, D.H., A.D. Startsev, and H. Nguyen (2001). "Soil Wetness and Traffic Level Effects on Bulk Density and Air-Filled Porosity of Compacted Boreal Forest Soils". *Soil Science Society of America Journal* 65.4, pp. 1238–1247. doi: 10.2136/sssaj2001.6541238x.
- Melling, Lulie (2016). "Peatland in Malaysia". *Tropical Peatland Ecosystems*. Ed. by Mitsuru Osaki and Nobuyuki Tsuji. Tokyo: Springer Japan, pp. 59–73. doi: 10.1007/978-4-431-55681-7\_4.
- Melling, Lulie, Kah Joo Goh, Auldry Chaddy, and Ryusuke Hatano (2014). "Soil CO<sub>2</sub> Fluxes from Different Ages of Oil Palm in Tropical Peatland of Sarawak, Malaysia". *Soil Carbon*. Ed. by Alfred E. Hartemink and Kevin McSweeney. Cham: Springer International Publishing, pp. 447–455. doi: 10.1007/978-3-319-04084-4\_44.
- Mesri, G., T. D. Stark, M. A. Ajlouni, and C. S. Chen (1997). "Secondary Compression of Peat with or without Surcharging". *Journal of Geotechnical and Geoenvironmental Engineering* 123.5, pp. 411–421. doi: 10.1061/(ASCE)1090-0241(1997)123:5(411).
- Mordhorst, A., S. Peth, and R. Horn (2014). "Influence of mechanical loading on static and dynamic CO<sub>2</sub> efflux on differently textured and managed Luvisols". *Geoderma* 219-220, pp. 1–13. doi: 10.1016/j.geoderma.2013.12.020.
- Murdiyarso, D., K. Hergoualc'h, and L. V. Verchot (2010). "Opportunities for reducing greenhouse gas emissions in tropical peatlands". *Proceedings of the National Academy of Sciences* 107.46, pp. 19655–19660. doi: 10.1073/pnas.0911966107.

- Nawaz, Muhammad Farrakh, Guilhem Bourrié, and Fabienne Trolard (2013). "Soil compaction impact and modelling. A review". *Agronomy for Sustainable Development* 33.2, pp. 291–309. doi: 10.1007/s13593-011-0071-8.
- Norberg, Lisbet (2017). "Greenhouse Gas Emissions from Cultivated Organic Soils". *Doctoral thesis, Sveriges lantbruksuniversitetet, Acta Universitatis Agriculturae Sueciae*, ISBN 978-91-576-8833-0, pp. 1–62.
- O'Sullivan, M (1996). "Critical state parameters from intact samples of two agricultural topsoils". *Soil and Tillage Research* 39.3-4, pp. 161–173. doi: 10.1016/S0167-1987(96)01068-9.
- Ogle, D.H., J.C. Doll, P. Wheeler, and A. Dinno (2021). *FSA: Fisheries Stock Analysis*. url: <https://github.com/droglenc/FSA>.
- Othman, Hasnol, Farawahida Mohamad Darus, and Ahmad Tarmizi (2009). "Experiences in Peat Development for Oil Palm Planting in the MPOB Research Station at Sessang, Sarawak", pp. 1–13.
- Page, S.E. and A.J. Baird (2016). "Peatlands and Global Change: Response and Resilience". *Annual Review of Environment and Resources* 41.1, pp. 35–57. doi: 10.1146/annurev-environ-110615-085520.
- Pihlatie, Mari, Eija Syväsalö, Asko Simojoki, Martti Esala, and Kristiina Regina (2004). "Contribution of nitrification and denitrification to N<sub>2</sub>O production in peat, clay and loamy sand soils under different soil moisture conditions". *Nutrient Cycling in Agroecosystems* 70.2, pp. 135–141. doi: 10.1023/B:FRES.0000048475.81211.3c.
- Pinheiro, Jose, Douglas Bates, Saikat DebRoy, and Deepayan Sarkar (2020). *nlme: Linear and Nonlinear Mixed Effects Models*. url: <https://CRAN.R-project.org/package=nlme>.
- R Core Team (2020). *R: A language and environment for statistical computing*. Vienna, Austria. url: <https://www.R-project.org/>.
- Rahman, Aatur, Azmi Yahya, Mohd. Zodaïdie, Desa Ahmad, Wan Ishak, and A.F. Kheiralla (2004). "Mechanical properties in relation to vehicle mobility of Sepang peat terrain in Malaysia". *Journal of Terramechanics* 41.1, pp. 25–40. doi: 10.1016/j.jterra.2004.01.002.
- Reichert, José Miguel, Luis Eduardo Akiyoshi Sanches Suzuki, Dalvan José Reinert, Rainer Horn, and Inge Håkansson (2009). "Reference bulk density and critical degree-of-compactness for no-till crop production in subtropical highly weathered soils". *Soil and Tillage Research* 102.2, pp. 242–254. doi: 10.1016/j.still.2008.07.002.

- Ruser, R., H. Flessa, R. Russow, G. Schmidt, F. Buegger, and J.C. Munch (2006). "Emission of N<sub>2</sub>O, N<sub>2</sub> and CO<sub>2</sub> from soil fertilized with nitrate: effect of compaction, soil moisture and rewetting". *Soil Biology and Biochemistry* 38.2, pp. 263–274. doi: 10.1016/j.soilbio.2005.05.005.
- Ruser, R., R. Schilling, H. Steindl, H. Flessa, and F. Beese (1998). "Soil Compaction and Fertilization Effects on Nitrous Oxide and Methane Fluxes in Potato Fields". *Soil Science Society of America Journal* 62.6, pp. 1587–1595. doi: 10.2136/sssaj1998.03615995006200060016x.
- Ryan, Michael G. and Beverly E. Law (2005). "Interpreting, measuring, and modeling soil respiration". *Biogeochemistry* 73.1, pp. 3–27. doi: 10.1007/s10533-004-5167-7.
- Säurich, Annelie, Bärbel Tiemeyer, Ullrich Dettmann, and Axel Don (2019). "How do sand addition, soil moisture and nutrient status influence greenhouse gas fluxes from drained organic soils?" *Soil Biology and Biochemistry* 135, pp. 71–84. doi: 10.1016/j.soilbio.2019.04.013.
- Sitaula, B.K., S. Hansen, J.I.B. Sitaula, and L.R. Bakken (2000). "Effects of soil compaction on N<sub>2</sub>O emission in agricultural soil". *Chemosphere - Global Change Science* 2.3-4, pp. 367–371. doi: 10.1016/S1465-9972(00)00040-4.
- Sognnes, Liv S., Gustav Fystro, Samson L. Øpstad, Arve Arstein, and Trond Børresen (2006). "Effects of adding moraine soil or shell sand into peat soil on physical properties and grass yield in western Norway". *Acta Agriculturae Scandinavica, Section B - Plant Soil Science* 56.3, pp. 161–170. doi: 10.1080/09064710500218845.
- Stolte, Jannes, Mehreteab Tesfai, Lillian Øygarden, Sigrun Kværnø, Jacob Keizer, Frank Verheijen, Panos Panagos, Cristiano Ballabio, and Rudi Hessel (2015). *Soil threats in Europe*. EUR 27607 EN. Luxembourg: Publications Office.
- Teepe, Robert, Rainer Brumme, Friedrich Beese, and Bernard Ludwig (2004). "Nitrous Oxide Emission and Methane Consumption Following Compaction of Forest Soils". *Soil Science Society of America Journal* 68.2, pp. 605–611. doi: 10.2136/sssaj2004.6050.
- Tiemeyer, Bärbel, Elisa Albiac Borraz, Jürgen Augustin, Michel Bechtold, Sascha Beetz, Colja Beyer, Matthias Drösler, Martin Ebli, Tim Eickenscheidt, Sabine Fiedler, Christoph Förster, Annette Freibauer, Michael Giebels, Stephan Glatzel, Jan Heinichen, Mathias Hoffmann, Heinrich Höper, Gerald Jurasinski, Katharina Leiber-Sauheitl, Mandy Peichl-Brak, Niko Roßkopf, Michael Sommer, and Jutta Zeitz (2016). "High emissions of greenhouse gases from grasslands on peat and other organic soils". *Global Change Biology* 22.12, pp. 4134–4149. doi: 10.1111/gcb.13303.

- Ungureanu, N, V Vlăduț, Gh Voicu, S Șt Biriș, M Ionescu, M Dincă, D I Vlăduț, and M Matache (2016). "INFLUENCE OF WHEEL LOAD AND TIRE INFLATION PRESSURE ON FOOTPRINT AREA IN STATIC REGIME". 44. Symposium "Actual Tasks on Agricultural Engineering", Opatija, Croatia, 2016.631.431.73, pp. 99–110.
- Uusitalo, Jori and Jari Ala-Ilomäki (2013). "The significance of above-ground biomass, moisture content and mechanical properties of peat layer on the bearing capacity of ditched pine bogs". *Silva Fennica* 47.3. doi: 10.14214/sf.993.
- Vennik, Kersti, Peeter Kukk, Kadri Krebstein, Endla Reintam, and Thomas Keller (2019). "Measurements and simulations of rut depth due to single and multiple passes of a military vehicle on different soil types". *Soil and Tillage Research* 186, pp. 120–127. doi: 10.1016/j.still.2018.10.011.
- Verry, Elon S, Don H Boelter, Juhani Päivänen, Dale S Nichols, Tom Malterer, and Avi Gafni (2011). "Physical Properties of Organic Soils". *Peatland Biogeochemistry and Watershed Hydrology*, p. 42.
- Walczak, R, E Rovdan, and B Witkowska-Walczak (2002). "Water retention characteristics of peat and sand mixtures". *International Agrophysics* 16, pp. 161–165.
- Weisskopf, P., R. Reiser, J. Rek, and H.-R. Oberholzer (2010). "Effect of different compaction impacts and varying subsequent management practices on soil structure, air regime and microbiological parameters". *Soil and Tillage Research* 111.1, pp. 65–74. doi: 10.1016/j.still.2010.08.007.
- Wong, L.S., R. Hashim, and F.H. Ali (2009). "A Review on Hydraulic Conductivity and Compressibility of Peat". *Journal of Applied Sciences* 9.18, pp. 3207–3218. doi: 10.3923/jas.2009.3207.3218.
- Yamaguchi, Hareyuki, Yoshinori Ohira, Keiji Kogure, and Shigeru Mori (1985). "Undrained Shear Characteristics of Normally Consolidated Peat Under Triaxial Compression and Extension Conditions". *Soils and Foundations* 25.3, pp. 1–18. doi: 10.3208/sandf1972.25.3\_1.
- Yang, Z.X., C.F. Zhao, C.J. Xu, S.P. Wilkinson, Y.Q. Cai, and K. Pan (2016). "Modelling the engineering behaviour of fibrous peat formed due to rapid anthropogenic terrestrialization in Hangzhou, China". *Engineering Geology* 215, pp. 25–35. doi: 10.1016/j.enggeo.2016.10.009.
- Young, I.M and K Ritz (2000). "Tillage, habitat space and function of soil microbes". *Soil and Tillage Research* 53.3-4, pp. 201–213. doi: 10.1016/S0167-1987(99)00106-3.
- Zhang, Bin, Rainer Horn, and Paul D. Hallett (2005). "Mechanical Resilience of Degraded Soil Amended with Organic Matter". *Soil Science Society of America Journal* 69.3, pp. 864–871. doi: 10.2136/sssaj2003.0256.